
Electronic Theses and Dissertations, 2004-2019

2010

Conventional And Zvt Synchronous Buck Converter Design, Analysis, And Measurement

Mark Cory
University of Central Florida



Part of the [Electrical and Electronics Commons](#)

Find similar works at: <https://stars.library.ucf.edu/etd>

University of Central Florida Libraries <http://library.ucf.edu>

This Masters Thesis (Open Access) is brought to you for free and open access by STARS. It has been accepted for inclusion in Electronic Theses and Dissertations, 2004-2019 by an authorized administrator of STARS. For more information, please contact STARS@ucf.edu.

STARS Citation

Cory, Mark, "Conventional And Zvt Synchronous Buck Converter Design, Analysis, And Measurement" (2010). *Electronic Theses and Dissertations, 2004-2019*. 4407.

<https://stars.library.ucf.edu/etd/4407>



CONVENTIONAL AND ZVT SYNCHRONOUS BUCK CONVERTER
DESIGN, ANALYSIS, AND MEASUREMENT

by

MARK CORY
B.S. Electrical Engineering Purdue University, 2007

A thesis submitted in partial fulfillment of the requirements
for the degree of Master of Science in Electrical Engineering
in the School of Electrical Engineering and Computer Science
in the College of Engineering and Computer Science
at the University of Central Florida
Orlando, Florida

Spring Term 2010

ABSTRACT

The role played by power converting circuits is extremely important to almost any electronic system built today. Circuits that use converters of any type depend on power that is consistent in form and reliable in order to properly function. In addition, today's demands require more efficient use of energy, from large stationary systems such as power plants all the way down to small mobile devices such as laptops and cell phones. This places a need to reduce any losses to a minimum. The power conversion circuitry in a system is a very good place to reduce a large amount of unnecessary loss. This can be done using circuit topologies that are low loss in nature. For low loss and high performance, soft switching topologies have offered solutions in some cases.

Also, limited study has been performed on device ageing effects on switching mode power converting circuits. The impact of this effect on a converter's overall efficiency is theoretically known but with little experimental evidence in support.

In this thesis, non-isolated buck type switching converters will be the main focus. This type of power conversion is widely used in many systems for DC to DC voltage step down. Newer methods and topologies to raise converter power efficiency are discussed, including a new synchronous ZVT topology [1]. Also, a study has been performed on device ageing effects on converter efficiency. Various scenarios of voltage conversion, switching frequency, and circuit components as well as other conditions have been considered. Experimental testing has been performed in both cases, ZVT's benefits and device ageing effects, the results of which are discussed as well.

*Dedicated to my parents
John & Gayle Cory*

ACKNOWLEDGMENTS

Completing this thesis and the work associated with it would not have been possible without the help and support of others. I own much gratitude to those who helped me do so. The foundation of my work was, without a doubt, made more solid by the guidance, technical assistance, and emotional support of those around me. I wish to acknowledge all those who helped me throughout this process.

Firstly, I would like to thank my advisor and mentor Dr. Jiann Shiun Yuan for all of his help and guidance throughout my time at UCF. Dr. Yuan's help and direction greatly assisted me in my work. His guidance gave shape and structure to my work in this thesis. His great interest in the advancement of knowledge has given me inspiration to continue my educational pursuits to come. I truly appreciate all of his time and help.

I would also wish to display my gratitude to all the other professors and faculty that assisted in my continued education during my time at UCF as well as throughout my college carrier. I would also like to specifically thank Dr. Osama Abdel-Rahman for all of his help and extremely useful insight in the field of Power Electronics. Dr. Abdel-Rahman's teaching helped greatly in the advancement of my knowledge of Power Electronics. Thanks also to Dr. John Shen for the use of his laboratory and equipment as well as some of his insights into power devices.

Perhaps most importantly, I must thank all my friends and family for their love and support. I would like to thank my loving wife Allison L. Cory without whom I would not have been able to accomplish all that I have in school and in my life thus far. Allison I will always love you for all that you have sacrificed for me. To my parents John and Gayle, there are no words that are sufficient for me to use in order to thank you for all

that you have done for me throughout my life. I can never repay you for all of your love and support but I hope that I have made you proud up to this point and will strive always to do so.

TABLE OF CONTENTS

LIST OF FIGURES	ix
LIST OF TABLES	xi
LIST OF EQUATIONS	xii
CHAPTER 1: INTRODUCTION.....	1
1.1 Introduction	1
1.2 Objectives.....	2
1.3 Motivation	3
1.4 Thesis Structure.....	3
CHAPTER 2: BUCK CONVERTER BACKGROUND INFORMATION.....	4
2.1 Power Conversion	4
2.1.1 Purpose.....	4
2.1.2 Switching Mode Power Supplies	5
2.1.3 Loss and Efficiency.....	5
2.2 Non-Isolated Buck Converters	6
2.2.1 Description	6
2.2.2 Standard PWM Topology	6
2.2.3 Synchronous PWM Switching.....	12
2.3 Converter Losses	14
2.3.1 Losses in General.....	14
2.3.2 Switching Element Loss	15
2.3.2.1 Conduction Losses.....	15
2.3.2.2 Switching Losses	16

2.3.3	Other Loss	17
CHAPTER 3: NON-ISOLATED ZVT BUCK CONVERTER STUDY		19
3.1	Introduction	19
3.2	ZVS, ZCS, & ZVT Description	20
3.2.1	ZVS/ ZCS.....	21
3.2.2	ZVT.....	23
3.3	Synchronous ZVT Topology of Interest	27
3.3.1	Description and Reasoning	27
3.3.2	Operational Simulation	28
3.3.3	Design Considerations	32
3.4	Results/ Discussion	33
3.4.1	Standard Buck Converters	34
3.4.2	Synchronous ZVT Topology	39
3.5	Conclusions	50
3.6	Integrated Converter Discussion	51
CHAPTER 4: NON-ISOLATED SYNCHRONOUS BUCK CONVERTER STRESS EFFECTS.....		53
4.1	Introduction	53
4.2	Hot Electron Device Degradation	54
4.2.1	Description	54
4.2.2	Effects on Device Characteristics	56
4.2.3	Effects Pertaining to Power Electronic Circuits	58
4.2.4	Power Device Structures.....	59

4.2.5	Modeling/ Simulating Effects	60
4.3	Susceptibility of Converters	61
4.4	Experimental Simulation of Device Ageing	64
4.4.1	Methods of Stressing.....	64
4.4.2	Out of Circuit Stressing	64
4.4.3	In Circuit Stressing	66
4.5	Results/ Conclusions	67
CHAPTER 5: CONCLUSIONS AND FUTURE WORK.....		71
5.1	Conclusions	71
5.2	Future Work	71
REFERENCES		72

LIST OF FIGURES

Figure 1: Simplified Power Electronic System Block Diagram	2
Figure 2: Ideal PWM Buck Converter	6
Figure 3: Standard PWM Buck Converter Modes of Operation.....	7
Figure 4: CCM Operation	8
Figure 5: DCM Operation.....	9
Figure 6: DCM Operation Synchronous Switch with Negative Conduction.....	10
Figure 7: Ideal Synchronous Buck Converter.....	12
Figure 8: Dead Space Example.....	13
Figure 9: Ideal Synchronous Buck Converter Conduction Paths	14
Figure 10: Quasi-Resonant ZVS Buck Simulation Circuit.....	22
Figure 11: ZVS Switching Conditions.....	22
Figure 12: Conventional ZVT Buck Converter for Simulation	24
Figure 13: ZVT Converter ZVS Turn On.....	25
Figure 14: ZVT Converter ZVS Turn Off	26
Figure 15: ZVT Synchronous Buck Converter.....	27
Figure 16: Synchronous ZVT Topology Simulation Circuit	28
Figure 17: Synchronous ZVT Important Waveforms	29
Figure 18: Synchronous ZVT Converter Main Switch ZVS	30
Figure 19: Synchronous ZVT Converter Aux Switch ZCS	31
Figure 20: Standard Non-Synchronous Buck Converter Test Setup	35
Figure 21: Standard Synchronous Buck Converter Test Setup	36
Figure 22: Experimental Dead Space Control Waveforms.....	37

Figure 23: Synchronous Converter Board	37
Figure 24: Standard Buck Converters η vs. Pout Plots.....	38
Figure 25: Standard Buck Converters Power Loss vs. Pout Plots	39
Figure 26: Synchronous ZVT Converter Test Setup	40
Figure 27: Synchronous ZVT Converter Board.....	41
Figure 28: Synchronous ZVT Experimental Operational Waveforms	42
Figure 29: Auxiliary Switch ZCS Turn off Points.....	43
Figure 30: Synchronous ZVT vs. Synchronous buck Efficiency	44
Figure 31: Synchronous ZVT vs. Synchronous buck Power Loss	45
Figure 32: ZVT Efficiency with Auxiliary Component Improvement.....	46
Figure 33: ZVT Power Loss with Auxiliary Component Improvement.....	47
Figure 34: ZVT η Improvement in Reference to Synchronous Buck.....	47
Figure 35: ZVT Ploss Improvement in Reference to Synchronous Buck	48
Figure 36: Oxide Electron Trapping for Traditional MOSFET Structure	55
Figure 37: MOSFET Before and After Hot Carrier Ageing.....	57
Figure 38: LDMOS Before and After Hot Carrier Ageing.....	57
Figure 39: Example VDMOS Structure.....	59
Figure 40: Synchronous Buck Circuit for $\Delta R_{ds(on)}$ Simulation	62
Figure 41: $R_{ds(on)}$ Measurement Simulation Circuit.....	63
Figure 42: MOSFET Out of Circuit Stressing	65
Figure 43: Device $R_{ds(on)}$ Measurement Circuit.....	66
Figure 44: In Circuit Stressing Setup.....	67

LIST OF TABLES

Table 1: $\Delta\eta$ Due to ZCS Turn off Point.....	43
Table 2: Standard Synchronous Buck Converter Loss Estimation.....	49
Table 3: ZVT Synchronous Buck Converter Loss Estimation	49
Table 4: Simulated $\Delta R_{ds(on)}$ Impact on Efficiencies.....	63
Table 5: Theoretical $\Delta\eta$ due to $\Delta R_{ds(on)}$	68
Table 6: $R_{ds(on)}$ Before and After Stress (STP22NF03L).....	70

LIST OF EQUATIONS

Equation 1:	$V_{out} = D \cdot V_{in}$	7
Equation 2:	$T_{SW} = \frac{1}{F_{SW}}$	10
Equation 3:	$L_{crit} = \left(\frac{1-D}{2}\right) \cdot T_{SW} \cdot R$	11
Equation 4:	$\frac{\Delta V_{out}}{V_{out}} = \frac{1-D}{8 \cdot I_{out} \cdot C_{out} \cdot F_{SW}^2}$	11
Equation 5:	$P_{MOSFET} = P_{SW} + P_{COND}$	15
Equation 6:	$P_{CONDHS} = I_{OUT}^2 \cdot R_{DS(on)} \cdot D$	15
Equation 7:	$P_{CONDLS} = I_{OUT}^2 \cdot R_{DS(on)} \cdot (1 - D)$	16
Equation 8:	$P_{SW(HS)} = \left(\frac{V_{in} \cdot I_{out}}{2}\right) \cdot (F_{SW}) \cdot (t_{S(L-H)} + t_{S(H-L)})$	16
Equation 9:	$t_{S(L-H)} = \frac{Q_{G(SW)}}{I_{DRIVER(L-H)}}$	16
Equation 10:	$t_{S(H-L)} = \frac{Q_{G(SW)}}{I_{DRIVER(H-L)}}$	16
Equation 11:	$P_{SW(LS)} = \left(t_2 \cdot V_F + t_3 \cdot \frac{V_F + I_{OUT} \cdot 1.1 \cdot R_{DS(on)}}{2}\right) \cdot I_{OUT} \cdot F_{SW}$	16
Equation 12:	$t_{2R} = K_{2R} \cdot (R_{DRIVER} + R_{GATE}) \cdot C_{ISS}$	16
Equation 13:	$K_{2R} = \ln\left(\frac{V_{DRIVE}}{V_{DRIVE} - V_{SP}}\right) - \ln\left(\frac{V_{DRIVE}}{V_{DRIVE} - V_{TH}}\right)$	17
Equation 14:	$t_{3R} = K_{3R} \cdot (R_{DRIVER} + R_{GATE}) \cdot C_{ISS}$	17
Equation 15:	$K_{3R} = \ln\left(\frac{V_{DRIVE}}{V_{DRIVE} - 0.9 \cdot V_{SPEC}}\right) - \ln\left(\frac{V_{DRIVE}}{V_{DRIVE} - V_{SP}}\right)$	17
Equation 16:	$P_{DIODE} = t_{DEADTIME} \cdot F_{SW} \cdot V_F \cdot I_{OUT}$	17
Equation 17:	$\omega = \frac{1}{\sqrt{L_r \cdot C_r}}$	32
Equation 18:	$i_{Lr}(t - t_0) = \frac{V_i}{Z} \text{Sin}\omega(t - t_0)$	33

Equation 19: $Z = \sqrt{\frac{L_r}{C_r}}$ 33

CHAPTER 1: INTRODUCTION

1.1 Introduction

The field of Power Electronics is very broad and contains components from several disciplines of electrical engineering. Being general, Power Electronics involves converting energy from one form to another [3]. Globally we are becoming more aware that energy is a precious commodity. Therefore the use of energy is becoming such that we want more for less, that is, more work done using less energy than before. In essence, in any system we want energy expended to do the desired job only with no additional energy expenditures for unwanted or unnecessary work. This concept of high efficiency is nothing new but the demand for it seems to be growing.

Most Power Electronic systems can be simplified into three general components the source, converter, and load (shown in the block diagram below). The source provides the input energy and the load uses that energy to perform the desired task. The load can be anything from a motor to a microprocessor or a combination of items. In some cases, only a source and a load make up the entire system. However, in most systems some form of conversion is needed to provide the load with correct form of energy it needs. Certainly energy savings in any system, given a source, can be made almost anywhere in the system. The converter, being central to the energy flow, can be one of the best places to reduce unwanted losses. The ideal converter does not have any losses and the power in

is equal to the power out. In any real converter this is not the case of course and there are losses. Reducing this loss to a minimum is necessary to have a high level of efficiency.



Figure 1: Simplified Power Electronic System Block Diagram

1.2 Objectives

THESIS MAIN OBJECTIVES

- Providing expanded knowledge of ZVT soft switching buck converters through application of theory, simulation and experimental testing.
 - Using this expanded knowledge and pointing it in a useful direction.
 - Investigation of this topologies potential use in integrated applications.
- Analyzing the impacts of device ageing on switching converters using theory and experimental testing.
 - Discuss the various factors that are associated with the effects or lack of effects in converters.

1.3 Motivation

Continued study of power converting circuits is important for improving the performance and reliability of tomorrow's converters and by extension, the performance in terms of power consumption and overall reliability of the systems that they support. It is with this goal in mind that the research and experimental testing outlined in this paper was performed.

1.4 Thesis Structure

This thesis is structured as follows. In chapter 2, some foundation for the work to follow will be provided in the form of some basic knowledge and principals. Chapter 2 contains some fundamental concepts that may be useful in understanding for those not as familiar to the field of Power Electronics. In chapter 3, the focus is on soft switching buck converters and the first main objective of this paper will be addressed. In chapter 4, the focus is shifted to converter ageing effects and the second main objective of this paper will be addressed. In chapter 5, results from previous chapters will be noted and conclusions will be made based upon these results.

CHAPTER 2: BUCK CONVERTER BACKGROUND INFORMATION

2.1 Power Conversion

Power conversion is in and of itself a general topic, one that is addressed within the field of Power Electronics. There are four general forms of power converting circuits ac-to ac, ac-to-dc, dc-to ac, and dc to dc [3] [32]. Since addressing all forms of conversion would not be entirely useful for supporting the scope of the work done in this thesis, only dc-to-dc will be covered. Even within topic of dc-to-dc converters there are many circuit topologies and aspects of each circuit topology that can be addressed, the very thought of covering them all can be overwhelming. So, to simplify this and try to provide only what is necessary buck converters will be the main focus. This type of conversion is very often needed and it is one of the most popularly used.

2.1.1 Purpose

Power conversion in general is used to provide the correct form of energy needed by the load. Buck converters from a high level description provide a function that is very basic and necessary for many power systems. They step down the input voltage to a specified level and provide a level of regulation deemed necessary by the circuit.

2.1.2 Switching Mode Power Supplies

Buck type converters are switching mode power supplies, meaning that they use switching elements within their circuitry to manipulate the voltage and current characteristics of the output by using energy storage elements. This differs from a linear regulator that does not use switching elements and simply drops voltage by controlling a resistive element. The benefit of using a switch mode supply is in efficiency gain. This gain comes from the use of energy storage elements such as inductors and capacitors which ideally do not dissipate any energy. A buck converter can be thought of on an abstract level as a kind of DC transformer, in that it is used to change DC voltage and current characteristics from input to output similar to an AC transformer.

2.1.3 Loss and Efficiency

When using switching mode power electronic circuits, efficiency is always of some importance and often is very important. There can be other reasons, but generally a buck converter is used over a linear regulator mostly for the reason of higher efficiency. Lower losses and thus higher efficiency save power which is important for energy conservation. Energy conservation leads to beneficial results such as longer battery life, and reduced size for applications such as mobile electronic systems.

2.2 Non-Isolated Buck Converters

2.2.1 Description

The term non-isolated refers to the presence of a common voltage reference node between the input and output of the converter. The number of non-isolated buck converter topologies is still very large but by describing a couple of key topologies it becomes easier to understand some of the more complex ones.

2.2.2 Standard PWM Topology

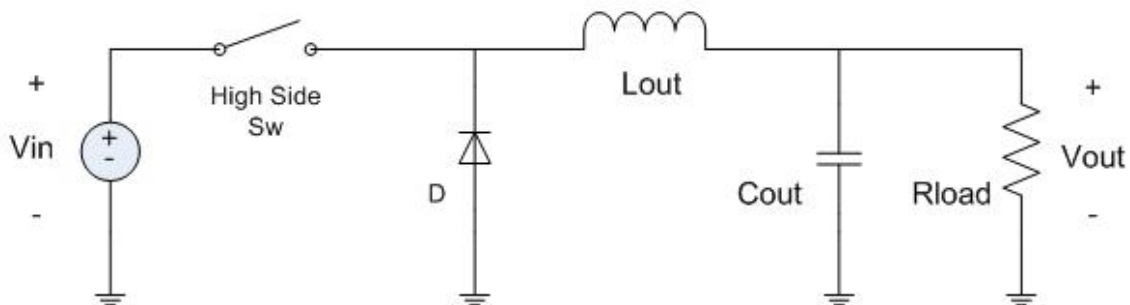


Figure 2: Ideal PWM Buck Converter

This is the most basic buck converter and its operation is very well known and thoroughly described in many texts [3] [32]. Since this is the case, the converter will be described qualitatively. See references such as [3] [32] for a more in depth description.

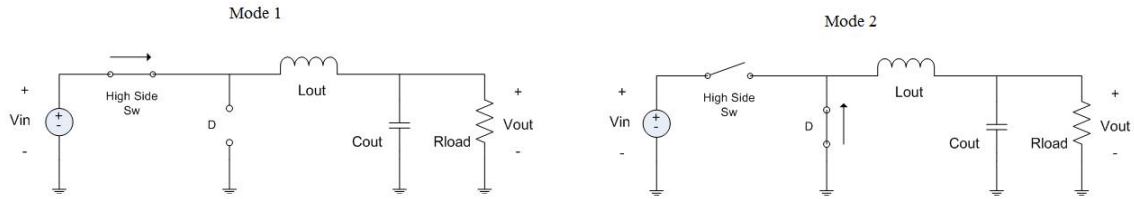


Figure 3: Standard PWM Buck Converter Modes of Operation

The duty cycle for the high side switch of this converter is used to control the output voltage with the following relation.

$$\text{Equation 1: } V_{out} = D \cdot V_{in}$$

This relation allows for what is known as PWM control. This method of control is preferred since it is easy to implement and very widely used. Another important aspect of this converter, to mention, is the inductor's conduction modes. This converter can operate in what is called constant conduction mode (CCM) or discontinuous conduction mode or (DCM) [3]. In CCM the inductor current is always greater than zero as in the figure below.

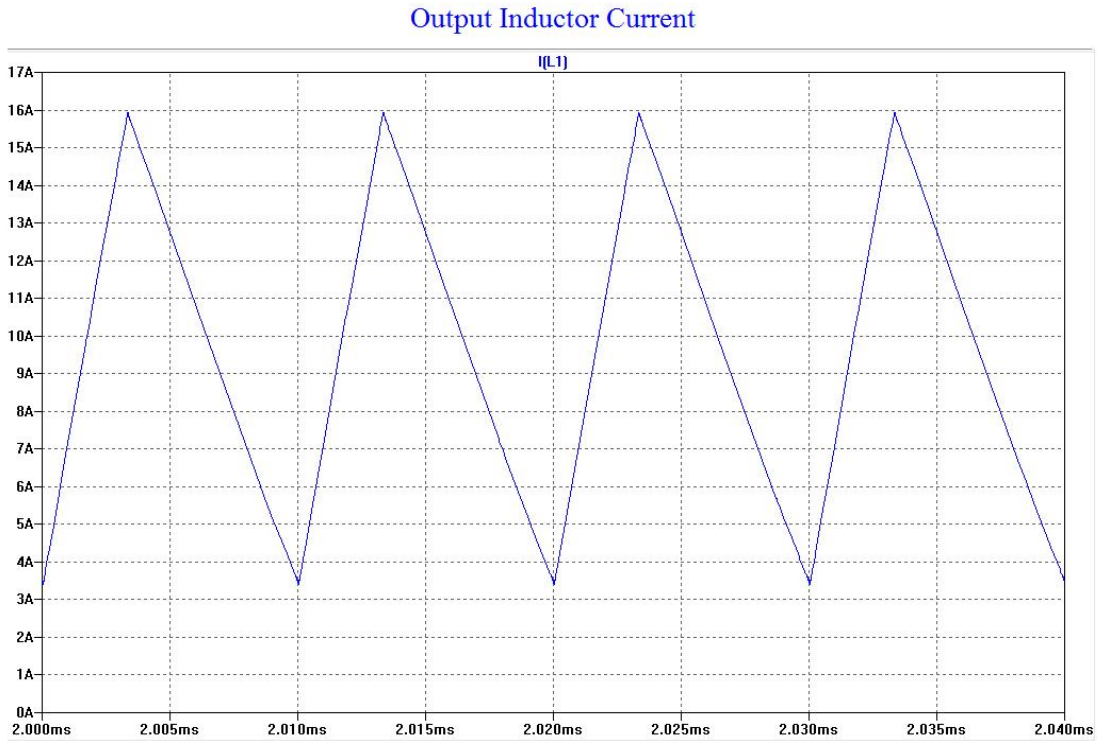


Figure 4: CCM Operation

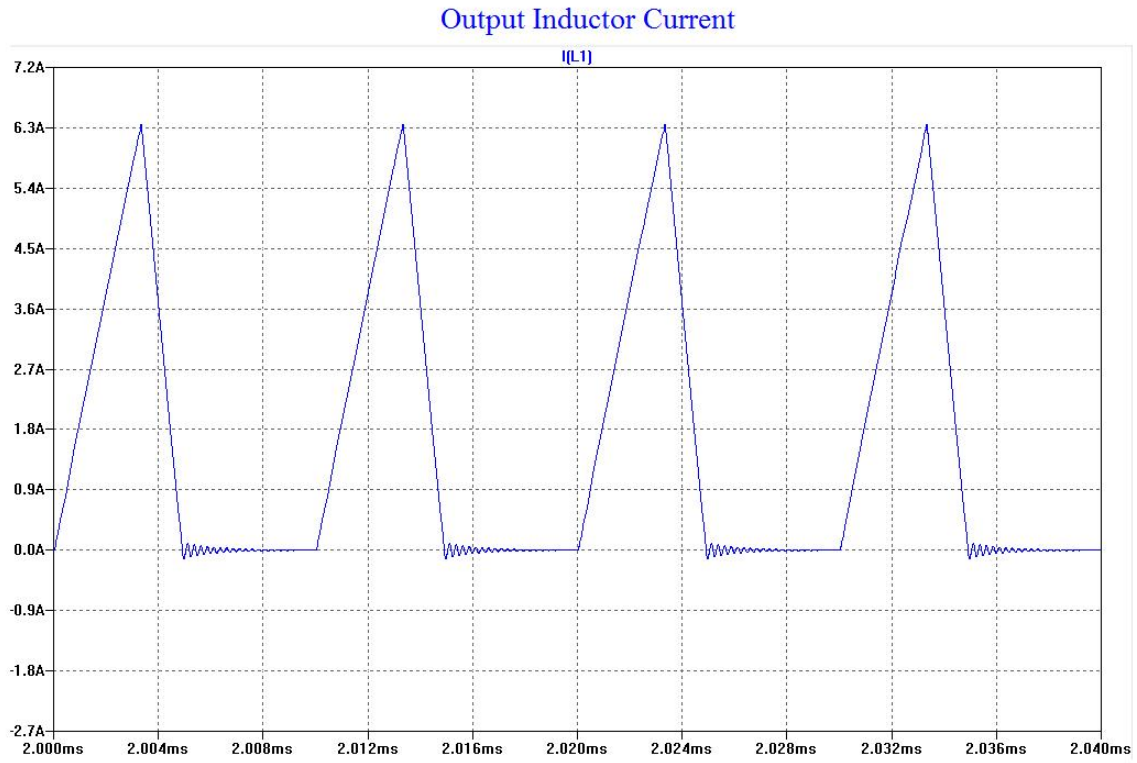


Figure 5: DCM Operation

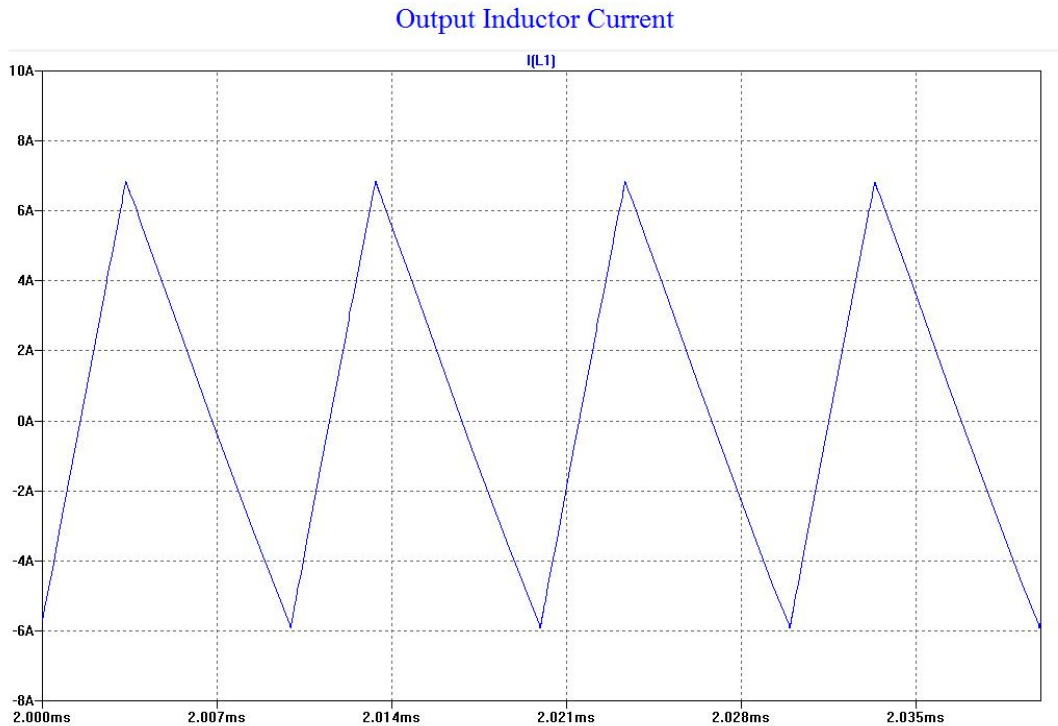


Figure 6: DCM Operation Synchronous Switch with Negative Conduction

In DCM operation the inductor current is zero for a portion of the switching period. Negative current is also possible if a synchronous switch is used depending on its control, as shown in the second DCM figure above. Which mode of inductor conduction the converter is in is controlled by output load level, switching frequency, duty cycle, and inductance (L_{out}). For a given switching frequency (F_{sw}), duty cycle (D), and load (R) there is what is called a critical inductance value (L_{crit}).

$$\text{Equation 2: } T_{sw} = \frac{1}{F_{sw}}$$

$$\text{Equation 3: } L_{crit} = \left(\frac{1-D}{2}\right) \cdot T_{sw} \cdot R$$

The conduction mode that the inductor is in is important for converter control and efficiency. Generally CCM is the preferred mode of converter operation since the converter gain is the simple linear relation as in equation 1. In DCM operation the gain (V_{out}/V_{in}) is not linear and equation 1 does not apply. For PWM controller design linear voltage gain is best. Also of importance is the magnitude of the voltage ripple generated at the converters output due to switching. This ripple is dependent on inductance (L_{out}), capacitance (C_{out}), duty cycle (D), and switching frequency (F_{sw}).

$$\text{Equation 4: } \frac{\Delta V_{out}}{V_{out}} = \frac{1-D}{8 \cdot L_{out} \cdot C_{out} \cdot F_{sw}^2}$$

The equations above are important to consider when designing any buck converter and although more advanced converters may not have the exact same relations the same general dependences on L_{out} , and C_{out} will remain.

2.2.3 Synchronous PWM Switching

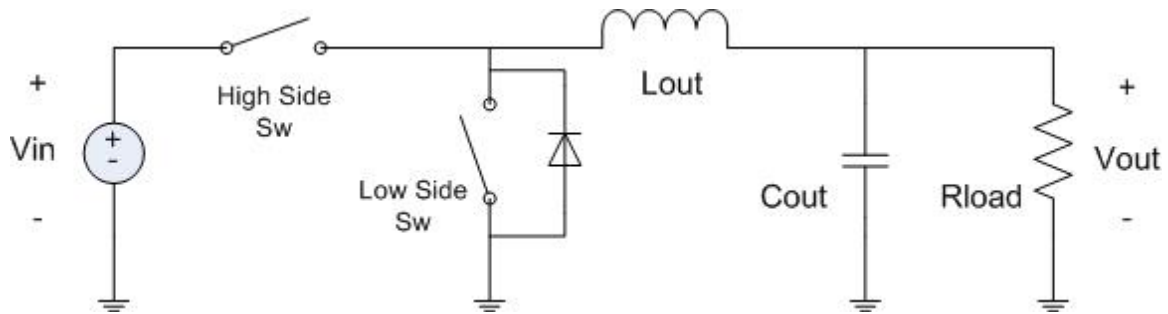


Figure 7: Ideal Synchronous Buck Converter

Synchronous switching is a method used to reduce converter losses by reducing the conduction losses sustained in the low side switching device. This means replacing the low side diode with a switching element such as a MOSFET. Diode losses due to the forward voltage drop of the p-n junction are greater than the channel conduction loss of a MOSFET. This is particularly beneficial for low duty cycles since more time is spent with the low side conducting, with some exceptions due to frequency of operation. This method adds some complexity to control but it is still PWM. Controlling this circuit requires two synchronous PWM signals that are inverted in comparison to each other with what is referred to as dead space or dead time between them.



Figure 8: Dead Space Example

This dead space is used to prevent the occurrence of a shoot through condition where there is a short circuit from V_{in} to ground causing high current spikes and large amounts of power loss. During this time either the body diode of the low side MOSFET is conducting or a separate parallel diode.

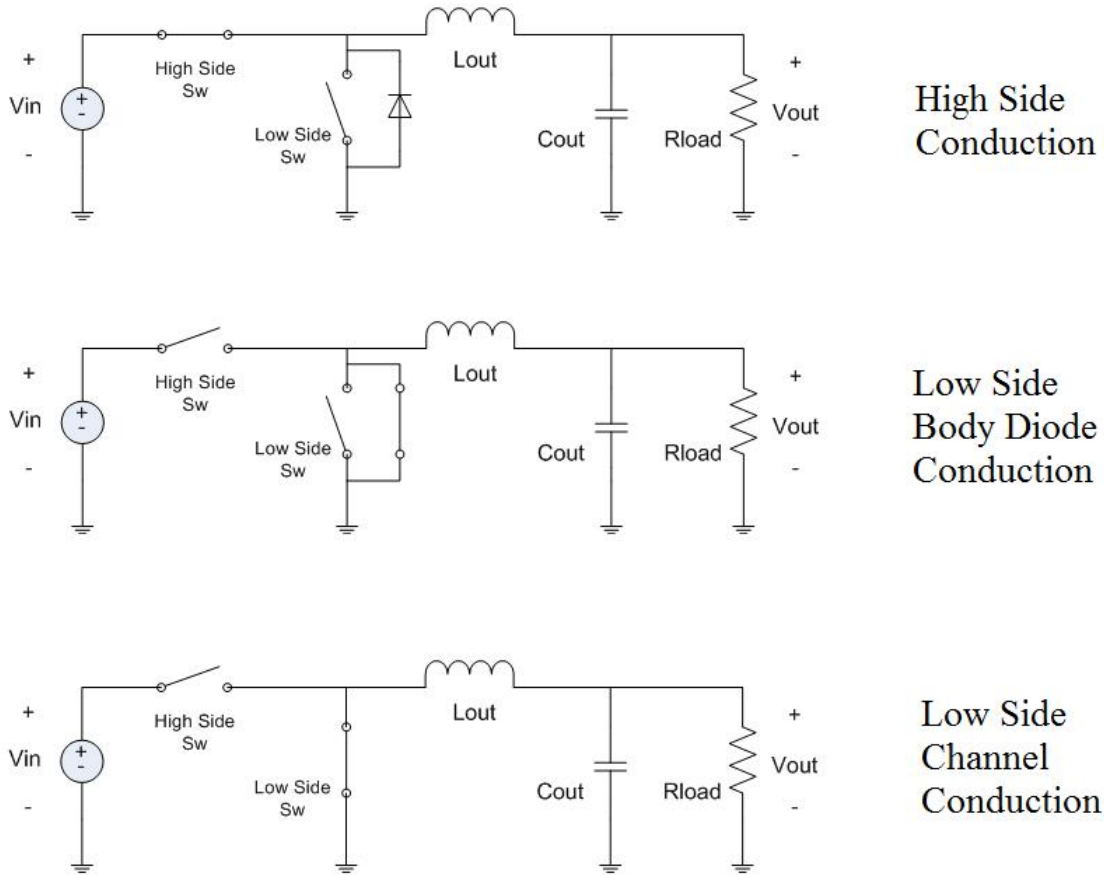


Figure 9: Ideal Synchronous Buck Converter Conduction Paths

2.3 Converter Losses

2.3.1 Losses in General

Losses can be found in any element of the converter. The amount of loss in each component depends on the element characteristics and the circuit operational characteristics. The distribution of loss can vary widely but typically switching elements

tend to remain of significant importance. However, the loss in other components cannot be overlooked.

2.3.2 *Switching Element Loss*

MOSFETs are very popularly used in most converters so it makes the most sense to use them in the description of switching element loss. The switch losses can be divided into two general forms of loss, conduction losses and switching losses. These losses are described in detail below [2]. The calculations used are approximations since the internal losses of every device cannot be measured during operation. This is a numerical method based on certain device characteristics with the synchronous buck converter in mind.

$$\text{Equation 5: } P_{MOSFET} = P_{SW} + P_{COND}$$

2.3.2.1 Conduction Losses

Conduction losses are defined as losses that are sustained due to the equivalent resistance of the MOSFET channel after the channel is completely enhanced. This resistance is the $R_{ds(on)}$ value for the transistor. Estimation of this loss can be made using the following equations for the high and low side devices.

$$\text{Equation 6: } P_{CONDHS} = I_{OUT}^2 \cdot R_{DS(on)} \cdot D$$

$$\text{Equation 7: } P_{CONDLS} = I_{OUT}^2 \cdot R_{DS(on)} \cdot (1 - D)$$

2.3.2.2 Switching Losses

Switching Losses occur during switching transitions as spikes in power are created due to rising voltage and falling current overlaps and vice versa depending on the transition occurring. In general these losses occur due to device parasitic capacitances. A good part of the switching losses sustained are due to the charging and discharging of these capacitances through larger resistance then are seen during device conduction. The equations used for estimation of these losses are below.

$$\text{Equation 8: } P_{SW(HS)} = \left(\frac{V_{in} \cdot I_{out}}{2} \right) \cdot (F_{SW}) \cdot (t_{S(L-H)} + t_{S(H-L)})$$

$$\text{Equation 9: } t_{S(L-H)} = \frac{Q_{G(SW)}}{I_{DRIVER(L-H)}}$$

$$\text{Equation 10: } t_{S(H-L)} = \frac{Q_{G(SW)}}{I_{DRIVER(H-L)}}$$

$$\text{Equation 11: } P_{SW(LS)} = \left(t_2 \cdot V_F + t_3 \cdot \frac{V_F + I_{OUT} \cdot 1.1 \cdot R_{DS(on)}}{2} \right) \cdot I_{OUT} \cdot F_{SW}$$

$$\text{Equation 12: } t_{2R} = K_{2R} \cdot (R_{DRIVER} + R_{GATE}) \cdot C_{ISS}$$

$$\text{Equation 13: } K_{2R} = \ln\left(\frac{V_{DRIVE}}{V_{DRIVE}-V_{SP}}\right) - \ln\left(\frac{V_{DRIVE}}{V_{DRIVE}-V_{TH}}\right)$$

$$\text{Equation 14: } t_{3R} = K_{3R} \cdot (R_{DRIVER} + R_{GATE}) \cdot C_{ISS}$$

$$\text{Equation 15: } K_{3R} = \ln\left(\frac{V_{DRIVE}}{V_{DRIVE}-0.9 \cdot V_{SPEC}}\right) - \ln\left(\frac{V_{DRIVE}}{V_{DRIVE}-V_{SP}}\right)$$

$$\text{Equation 16: } P_{DIODE} = t_{DEADTIME} \cdot F_{SW} \cdot V_F \cdot I_{OUT}$$

Note for the low side that equation 11 is used twice to calculate the rising and falling edge losses. Diode losses during dead space are included as switching losses as well with equation 16, these losses are often lumped with the low side switching losses since it typically is the low side MOSFET's body diode conducting. There are additional losses, due to the gate drive that are typically insignificant unless the switching frequency becomes extremely high, that not stated here [2].

2.3.3 *Other Loss*

Losses, as stated previously can be found in any element in the converter. Losses are found in both input and output capacitances due to the ESR (equivalent series resistance). Losses in the inductor (L_{out}) are in two forms those due to the DCR (direct current resistance) and core losses associated with the inductor core material. Any of these losses can become significant given the right conditions so they should not be

overlooked. Other additional losses such as control circuitry losses are typically small enough to be neglected. For upcoming converters to be discussed additional components are added, these components create loss that can be estimated similarly.

CHAPTER 3: NON-ISOLATED ZVT BUCK CONVERTER STUDY

3.1 Introduction

A large amount of work has been done on this topic since it was first introduced [15]. New topologies within this genre continue to spring up looking to improve upon this concept [1] [17-23] and move on to ever more efficient and power dense converters. To understand the work that has been done, some soft switching basic concepts must be explained. First of all, the reason soft switching is done in the first place needs to be understood. The next important thing to understand is how soft switching is accomplished. This leads into ZVT's contributions to this goal and looking more into the present, how newer ZVT topologies may help us better accomplish the goals of soft switching by improving upon this concept even further.

The driving force behind the development of soft switching topologies is the demand for high power density converters, which means more power handling capability in a smaller package. Typically a large amount of area used by a converter is occupied by the passive energy storage elements such as the output inductor and capacitor in a buck converter. This is due to the fact that for a given switching frequency, to reduce voltage and current ripple larger values of inductance and capacitance are used. Larger passive component values tend to be physically larger in size, thus taking up more area. To combat this for a given set of output voltage and load conditions the switching frequency can be increased allowing for the use of smaller component values. As switching frequency is increased so too are the converter's switching losses. At high frequencies switching losses can become the dominate loss in a converter. So the battle between

efficiency and area become more obvious. In order to save area high frequencies are desired, however at higher frequencies switching loss can cause a considerable drop in efficiency. Thus a creation of a need to reduce switching losses is present and soft switching topologies have sought to fulfill this need the best way possible.

3.2 ZVS, ZCS, & ZVT Description

Understanding how soft switching is accomplished is important in understanding how to use the topologies that achieve this goal. Soft switching topologies make use of additional circuit elements passive or active in order to limit di/dt or dv/dt during switching and minimize current and voltage overlap to reduce switching losses [30]. Essentially, in the switching device at the switching interval, either the current or the voltage must be driven to zero to bring the product of the two as close to zero as possible. This leads to the concepts of zero voltage switching (ZVS) and zero current switching (ZCS). Just as in the name either the voltage or current is driven to zero during switching. There are many topologies that use ZVS, ZCS, or both to reduce overall switching losses. Converters such as the ones termed as quasi-resonant can be used to achieve ZVS or ZCS [3] [16]. However, converters such as these can cause additional problems that offset soft switching benefits, such as additional voltage or current stress on the main switch [30]. Converters that have soft switching but reduce or eliminate this stress are more highly desirable. For this reason, what are known as zero voltage transition (ZVT) converters have become very popular and as stated previously, the number of ZVT topologies that have been introduced is large. ZVT converters accomplish soft switching while

minimizing additional stresses associated with other previous topologies. In the next two sub sections these concepts will be explained through examples.

3.2.1 ZVS/ ZCS

ZVS and ZCS switching topologies typically use resonance to bring the voltage or current in the switch to zero. In ZVS converters if a MOSFET is used, often this is accomplished by flowing current in the reverse direction through the body diode just before switching occurs, thus discharging the parallel capacitance of the switch bringing the voltage across it near zero before turn on. At turn off this parallel capacitance limits the dv/dt across the switch and causes a reduction current voltage overlap. In ZCS converters typically a resonance inductor placed in series with the switch is used to resonant the current through the switch to zero for turn off and limit di/dt for turn on [3] [16]. As an example of this simulation of a ZVS buck converter topology will be used below.

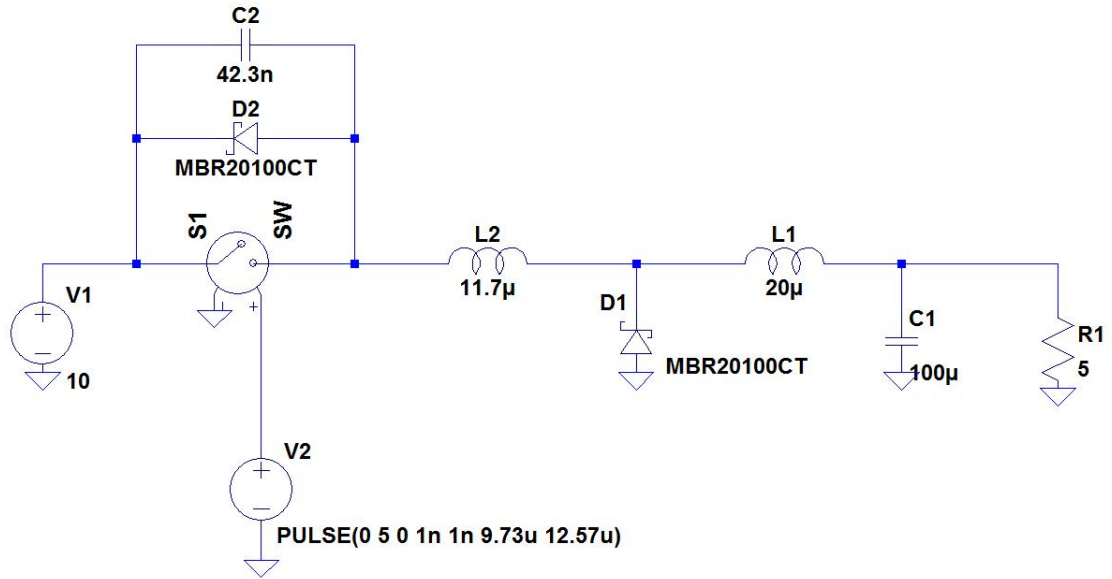


Figure 10: Quasi-Resonant ZVS Buck Simulation Circuit

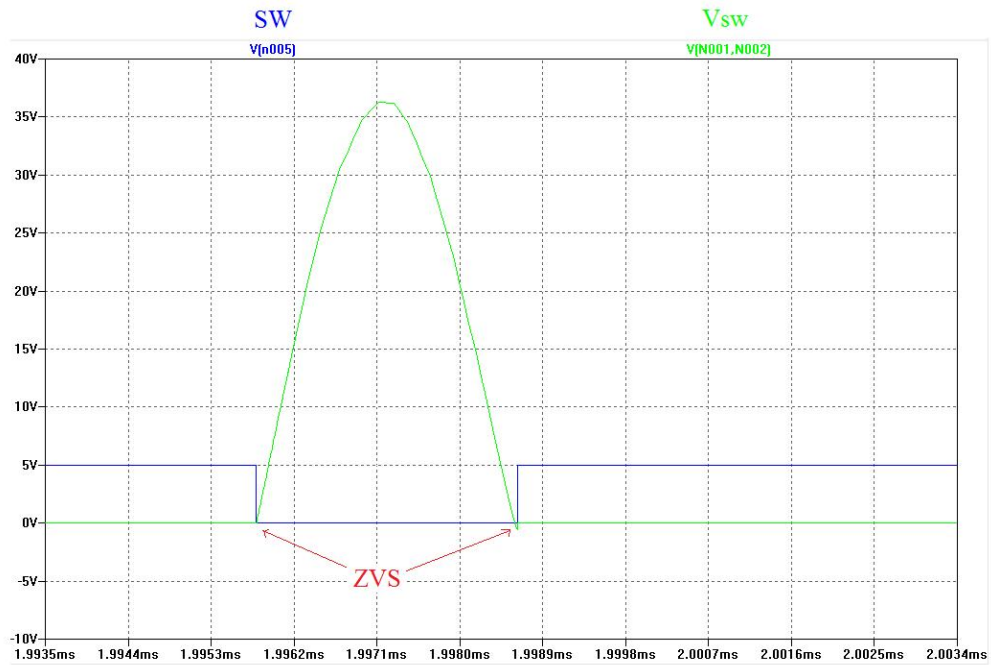


Figure 11: ZVS Switching Conditions

The circuit used in the above LTSpice simulation is based on a quasi-resonance type ZVS converter [3] [16]. The waveforms shown are the switch voltage in green (this would typically be the V_{ds} if a MOSFET were to replace the ideal switch) and the switching turn on and of waveform in blue (replace with V_{gs} for MOSFET). These waveforms demonstrate ZVS turn on and turn off for the switch. As can be seen a much larger voltage stress (approximately 3.6 times more) is applied across the switch than is seen for the standard PWM topology. This additional stress limits the devices that can be used to ones that typically have a larger $R_{ds(on)}$, thus creating more conduction losses. The additional conduction losses associated with this larger $R_{ds(on)}$ can offset any performance gains made by soft switching. Additionally this topology is a frequency modulated topology and not a PWM topology. This can cause some additional complications in implementation.

3.2.2 ZVT

There are many types of ZVT converters. This class of converters has been categorized more thoroughly into various types in [30]. However, in general there are two types of ZVT converters, ones that use passive auxiliary circuit elements only such as in [21] and ones that use active elements in the auxiliary circuit [1] [17-20] [23]. Active types will be the only ones discussed to follow. Although there are many different topologies that use ZVT the basic concept can be explained by using the buck topology from [15]. This family of topologies is typically considered to be the conventional ZVT

topologies. In this section ZVT will be explained using an example with this conventional ZVT buck converter. Below is simulation of this topology in LTSpice and its corresponding waveforms.

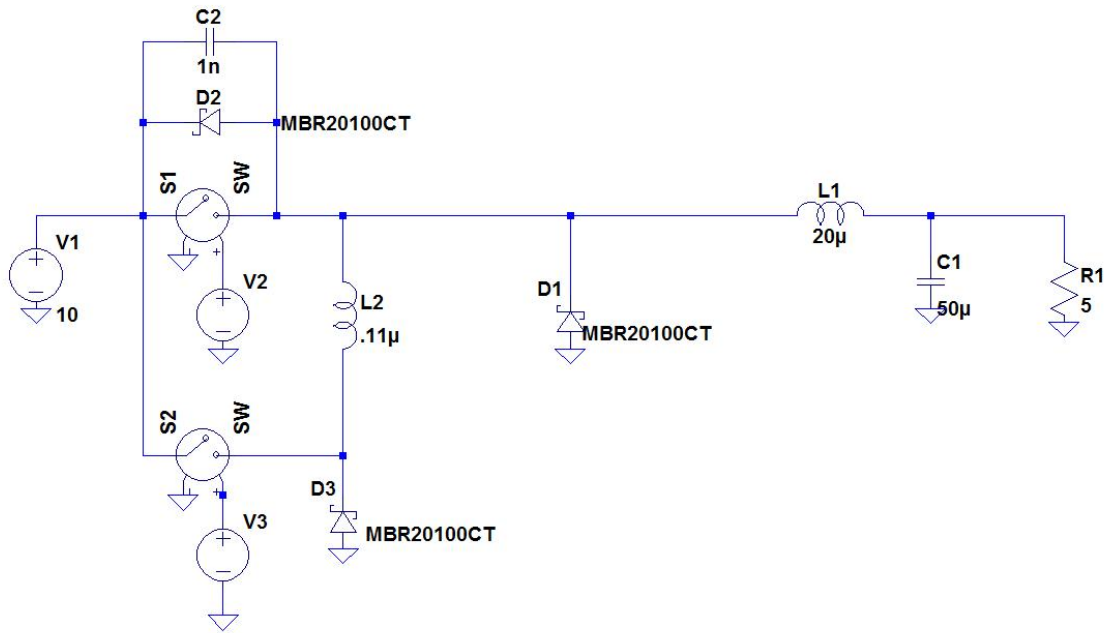


Figure 12: Conventional ZVT Buck Converter for Simulation

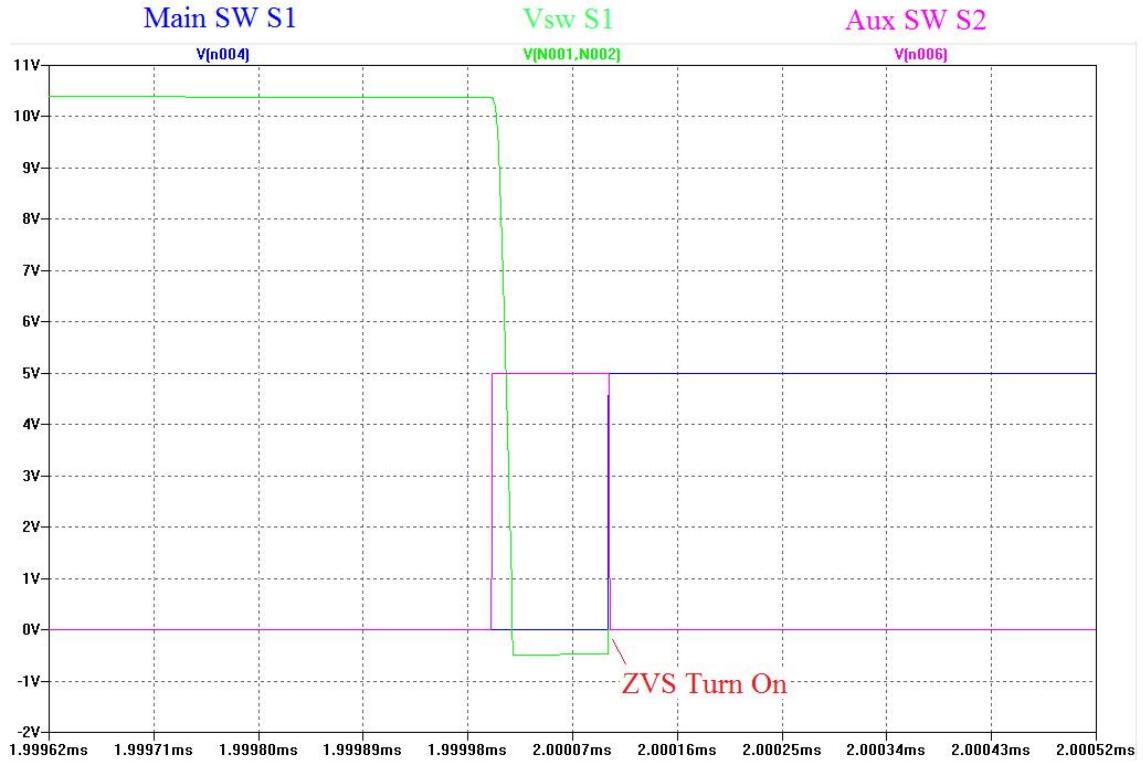


Figure 13: ZVT Converter ZVS Turn On



Figure 14: ZVT Converter ZVS Turn Off

The above simulation waveforms show that zero voltage turn on and off is achieved by this topology without inducing additional voltage stress on the main switch. This improvement allows for the use of lower rated switching elements that typically have lower $R_{ds(on)}$ values. However this topology is not without its drawbacks. The auxiliary switching elements induce some undesired losses, in particular there are still switching losses in the auxiliary switch. Hard switching in this switch creates additional switching losses that can lower the converters overall efficiency. Most recently ZVT topologies have turned their focus to include the elimination of switching losses in the

auxiliary switch as well, some even looking to virtually eliminate all losses associated with switching [1] [17-23].

3.3 Synchronous ZVT Topology of Interest

3.3.1 Description and Reasoning

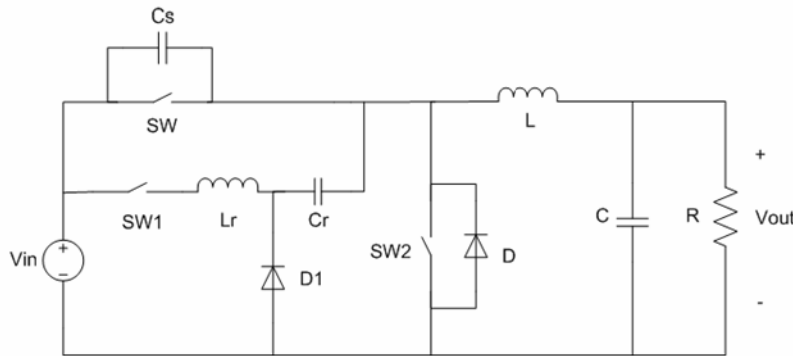


Figure 15: ZVT Synchronous Buck Converter

This converter topology is one that has recently been introduced into the category of ZVT switching converters [1]. This converter's operation allows for soft switching to occur in all switches used. This is a benefit not included in previous ZVT topologies such as [15]. Some of those that have included auxiliary switch soft switching, have added quite a large amount of complexity to the converter. This converter's design is fairly simplified when compared to others [17] [23]. This synchronous ZVT topology will be used for the analysis to follow. The main interest of ZVT is increase power density so it logically follows that this type of converter being low loss in nature and almost entirely

devoid of switching losses may be a candidate for use in application such as integration, similar to converters in [14] [24-27]. In order to see if this converter may be suitable for such applications further insight is required. It is with this interest in mind that the research done on this converter was carried out.

3.3.2 Operational Simulation

The operation of this converter is described in detail in [1]. Simulation was performed to show its operation in LTSpice.

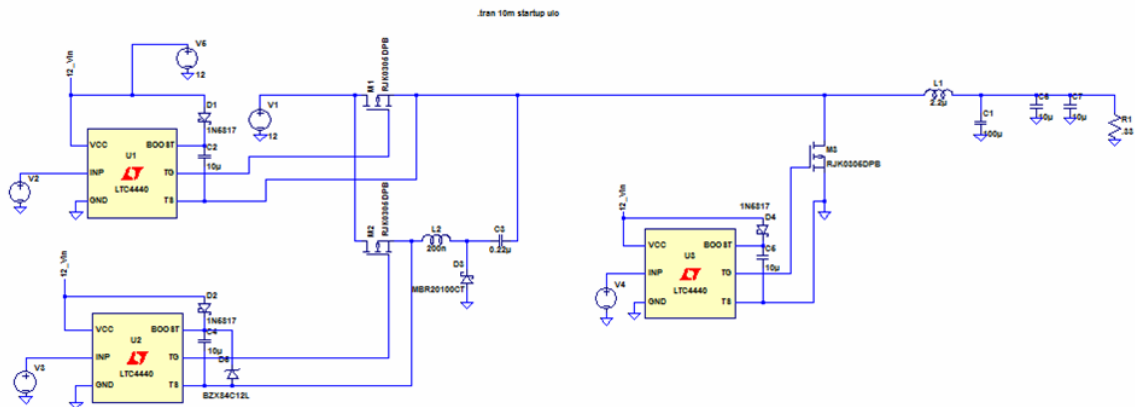


Figure 16: Synchronous ZVT Topology Simulation Circuit

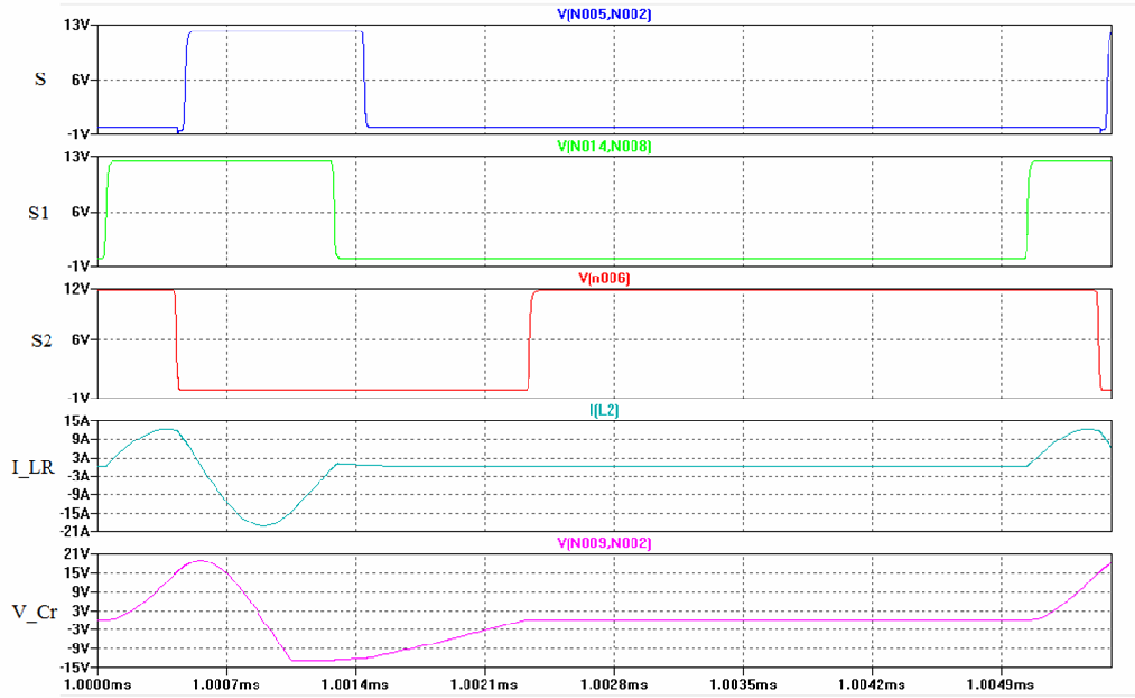


Figure 17: Synchronous ZVT Important Waveforms

The above operational waveforms are consistent with the ones described in [1] with one difference. The turn of switch one has been slightly delayed in order to improve the efficiency of the converter. This will be explained in the description to follow. Below are the switching waveforms confirming soft switching.

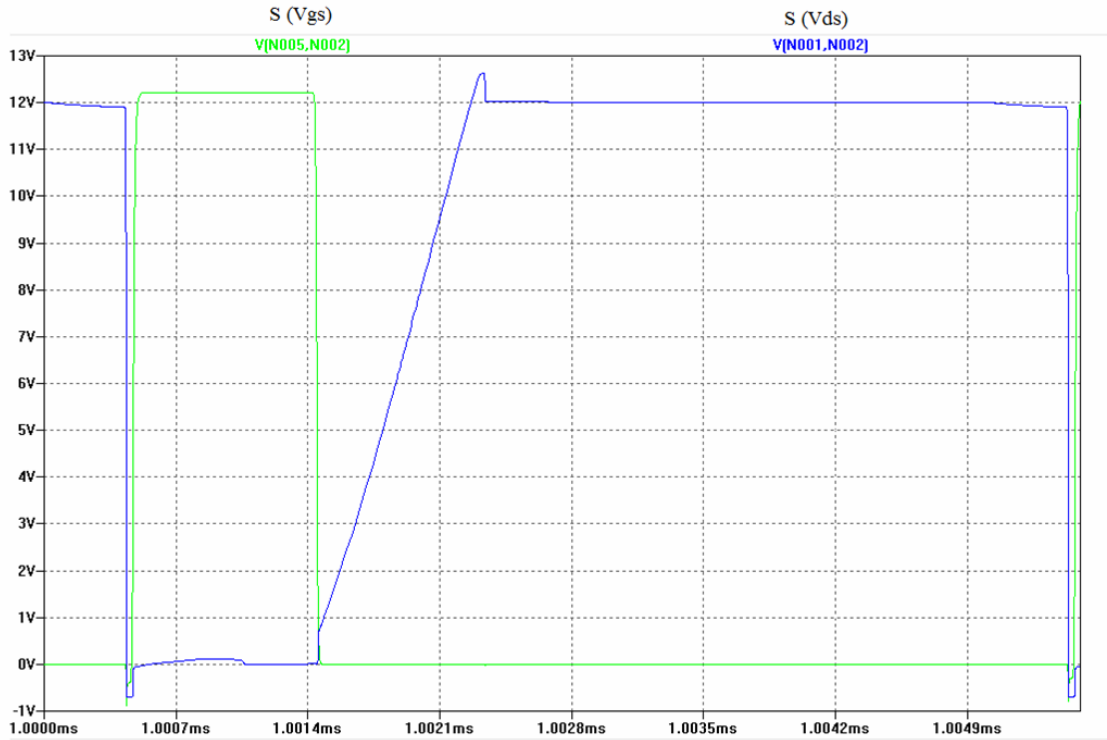


Figure 18: Synchronous ZVT Converter Main Switch ZVS

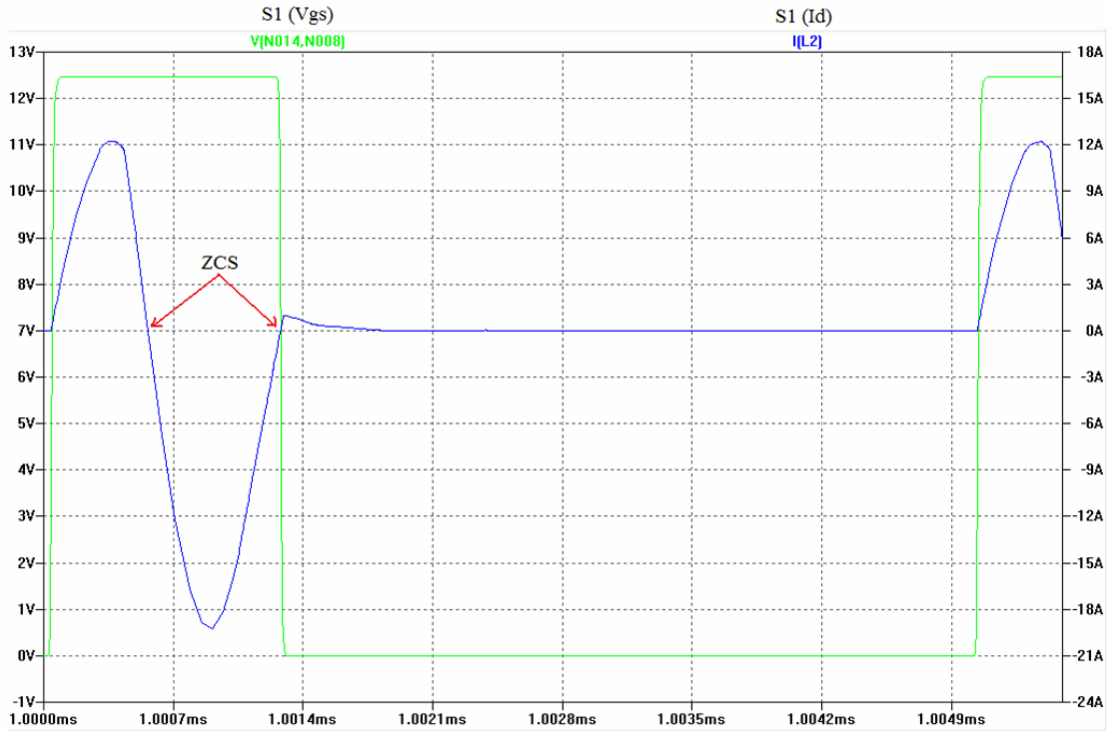


Figure 19: Synchronous ZVT Converter Aux Switch ZCS

As can be seen above soft switching occurs in both the main and auxiliary switches, in the form of ZVS for the main and ZCS for the auxiliary. As noted in the auxiliary switch figure above there are two opportunities to switch the auxiliary switch under ZCS conditions. In the description in [1] the auxiliary switch turns off at the first zero crossing allowing the body diode of the switch to conduct the resonance current in the negative direction. This creates more loss due to the forward drop of this body diode by leaving the switch turned on during this negative conduction period the current flows through the channel of the device which creates less loss similar to the use of a synchronous rectifier.

3.3.3 Design Considerations

ZVT Voltage and load testing conditions used for experimentation to follow were similar to those used in [1]. However, there are some important things to consider when using topology in general. First of all, as with other ZVT topologies the period of resonance between auxiliary components L_r and C_r should be small in comparison to the overall switching period. This is done in order to limit the auxiliary circuit's effects on gain and efficiency. PWM gain is still desired since it is linear and the smaller the resonance period is the more linear ZVT's gain is as well. Efficiency can also benefit from this as the smaller the time the auxiliary components spend conducting the smaller their conduction loss. The frequency and consequent resonance period of these auxiliary components is designed using the following equation.

$$\text{Equation 17: } \omega = \frac{1}{\sqrt{L_r \cdot C_r}}$$

Although this equation dictates the product of L_r and C_r the exact values of each are not specified by it. In order to pick the specific values of L_r and C_r input voltage and output load conditions must be considered. In order to accomplish ZVS soft switching in the main switch the magnitude of the resonance current through L_r must exceed the load output current. This is to induce the current flow through the device body diode necessary to create a ZVS turn on condition. Further detail is given in the circuit mode descriptions in [1] and can be used to better understand this concept. Below are the two equations used to determine the designed values of L_r and C_r .

$$\text{Equation 18: } i_{Lr}(t - t_0) = \frac{V_i}{Z} \text{Sin}\omega(t - t_0)$$

$$\text{Equation 19: } Z = \sqrt{\frac{L_r}{C_r}}$$

Equation 19 is the characteristic impedance. By using the equation for Lr resonance current (equation 18) it can be seen that for a given input voltage (Vin) the magnitude of this current can be controlled using the characteristic impedance (Z). This is important in the converter's design since the magnitude of resonance current essentially dictates the maximum load at which the converter is operating with complete soft switching conditions, keeping in mind that iLr should be greater than load current. There are several other design considerations, with most of the basic outlined in [1], but this is one of the most important. Proper timing of the switching waveforms is also important and must be considered in the design.

3.4 Results/ Discussion

This section includes a summary of the experimentation that was performed using this converter. This experimentation was carried out with the intention of being a platform for further investigation of this topology for application such as integration. Three converters were designed, built, and tested both standard synchronous and non-synchronous buck converters as well as the ZVT synchronous buck converter. Efficiency versus load data was taken for all three converters.

Some additional details are stated to eliminate any confusion. Parts used were kept as consistent as possible between converters in order to make as fair a comparison as possible. All converters were driven with an external bread boarded PWM. Gate drivers for switches were on board. Control was open loop and waveform timing was adjusted manually via potentiometer controls. This was done to allow for maximum adjustability of the converters in terms of waveform control, power stage components, conversion levels, and load conditions. Since converter characteristics were so dynamic, design of closed loop controls would have proved restrictive and time consuming. Voltage conversion for all converters to follow is from 12V to 3.3V unless otherwise noted. Any differences in converter setups should be noted on the particular setup as they are described.

3.4.1 Standard Buck Converters

To serve as a baseline for efficiency both synchronous and non-synchronous standard (hard switching) converters were built and tested. The test setup for both converters is shown below.

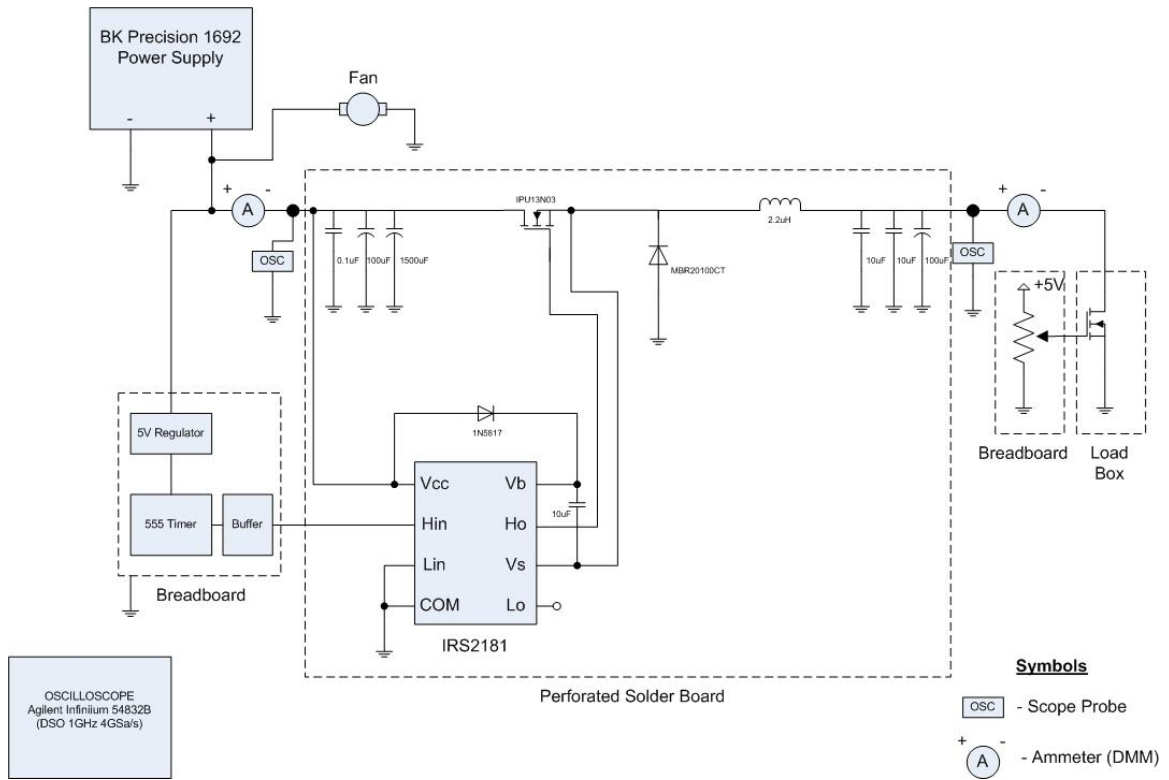


Figure 20: Standard Non-Synchronous Buck Converter Test Setup

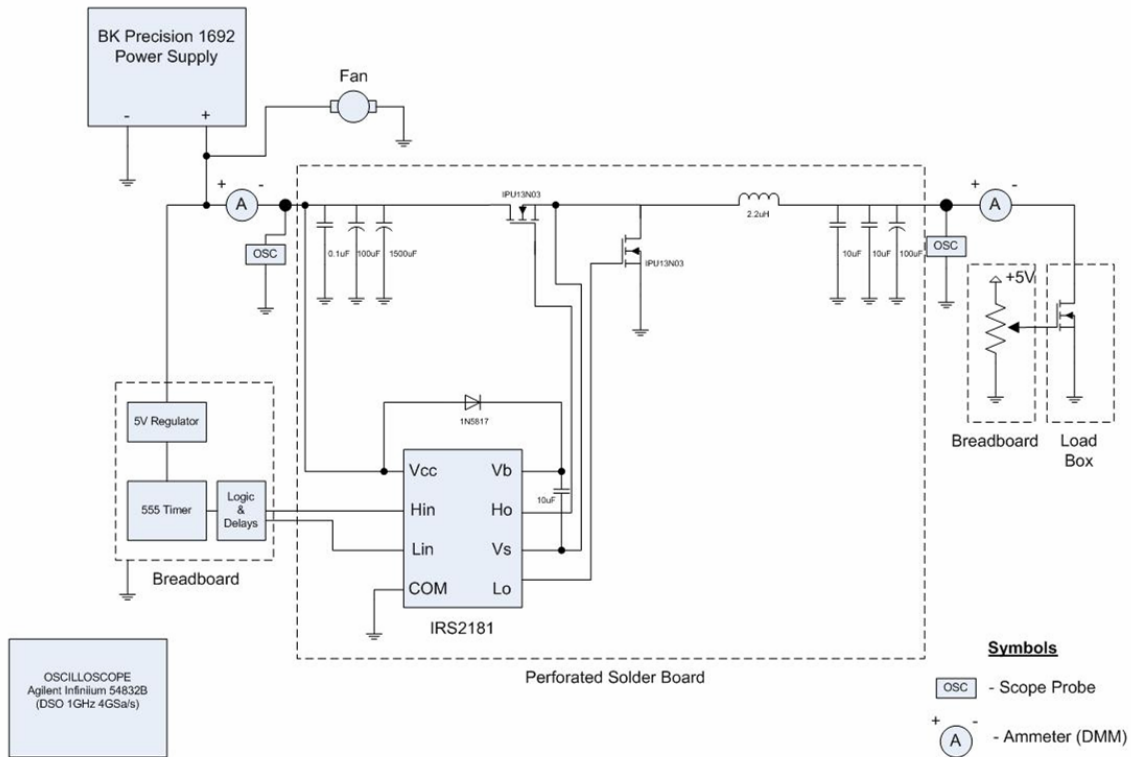
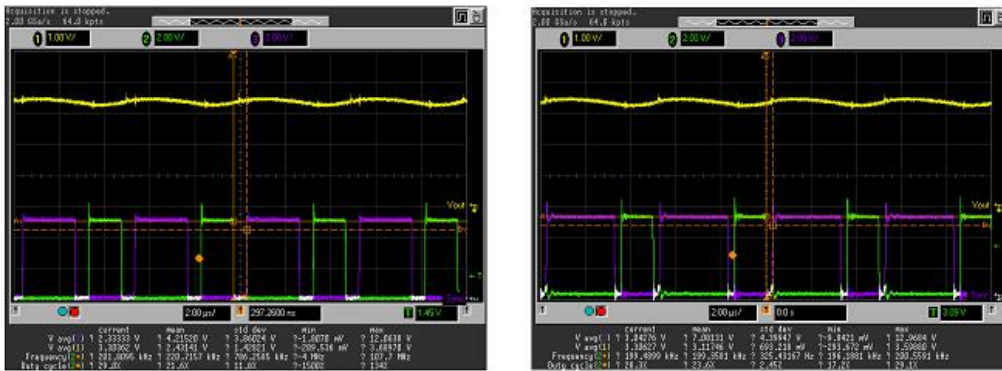


Figure 21: Standard Synchronous Buck Converter Test Setup

There is an adjustability factor for the synchronous converter that can make quite a bit of difference in efficiency results. This factor is the amount of dead space between the high side switch and the synchronous rectifier V_{gs} waveforms. Waveforms showing operation of the synchronous converter at two “ t_{dead} ” values of 600ns and 300ns while operating at a switching frequency of 200 kHz are shown below.

3A Load



$t_{dead} = 600\text{ns}$

$t_{dead} = 300\text{ns}$

Figure 22: Experimental Dead Space Control Waveforms

A picture of the actual synchronous converter board is shown below indicating the test points used for input and output voltages.

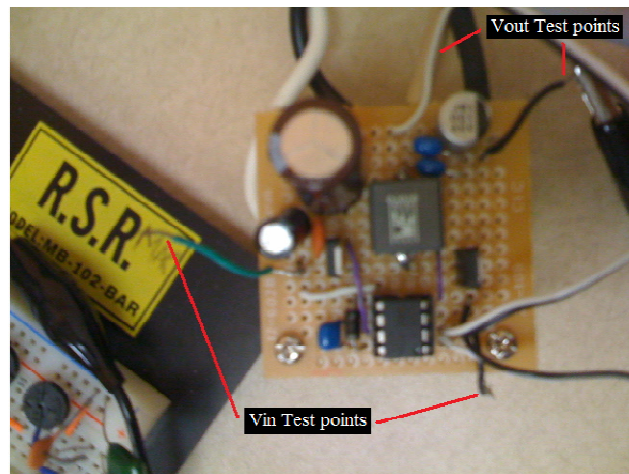


Figure 23: Synchronous Converter Board

Experimental results were obtained for these converters at an operating frequency of 200 kHz. The experimental results for efficiency testing of these converters are summarized in the efficiency and power loss plots below. The results are consistent with what is expected.

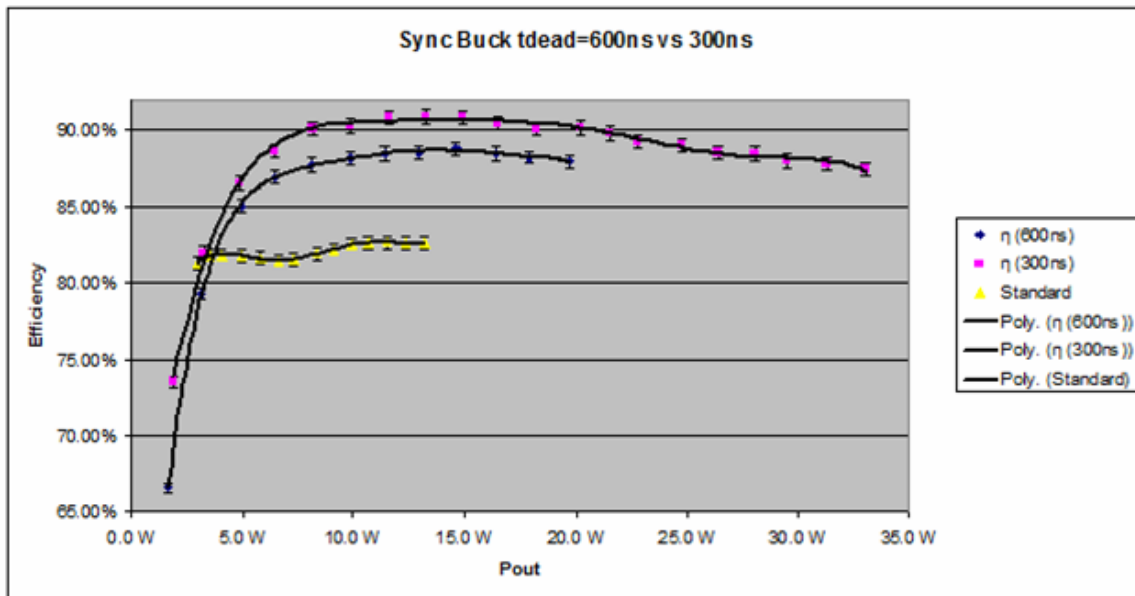


Figure 24: Standard Buck Converters η vs. Pout Plots

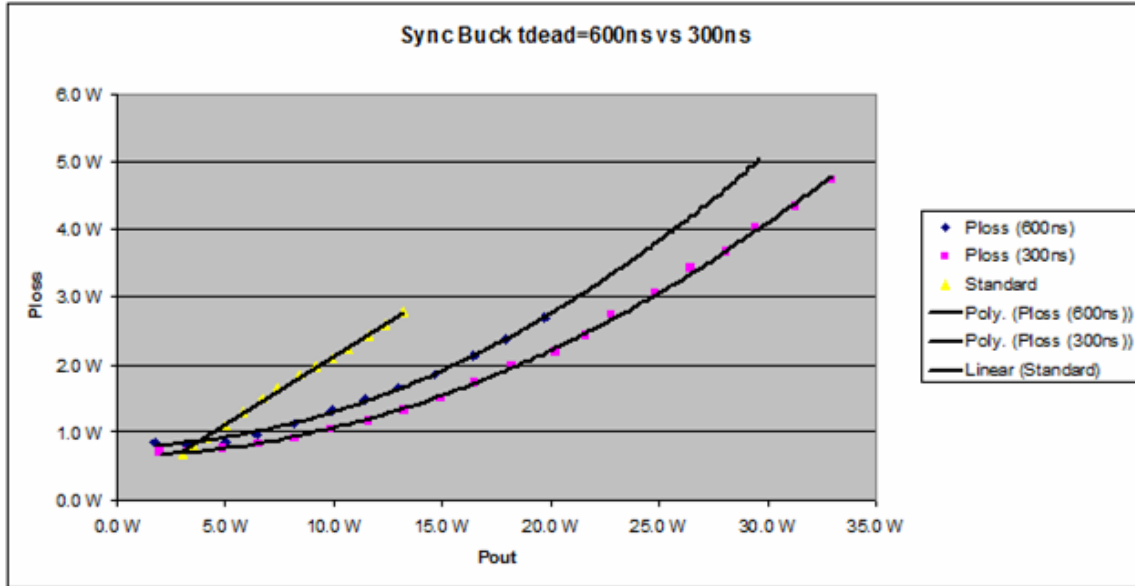


Figure 25: Standard Buck Converters Power Loss vs. Pout Plots

3.4.2 Synchronous ZVT Topology

The synchronous ZVT converter was built using the same main switching components as the standard buck converters (MOSFET part IPU13N03) but of course additional components were needed to serve as the auxiliary circuit components. Its test setup is shown below.

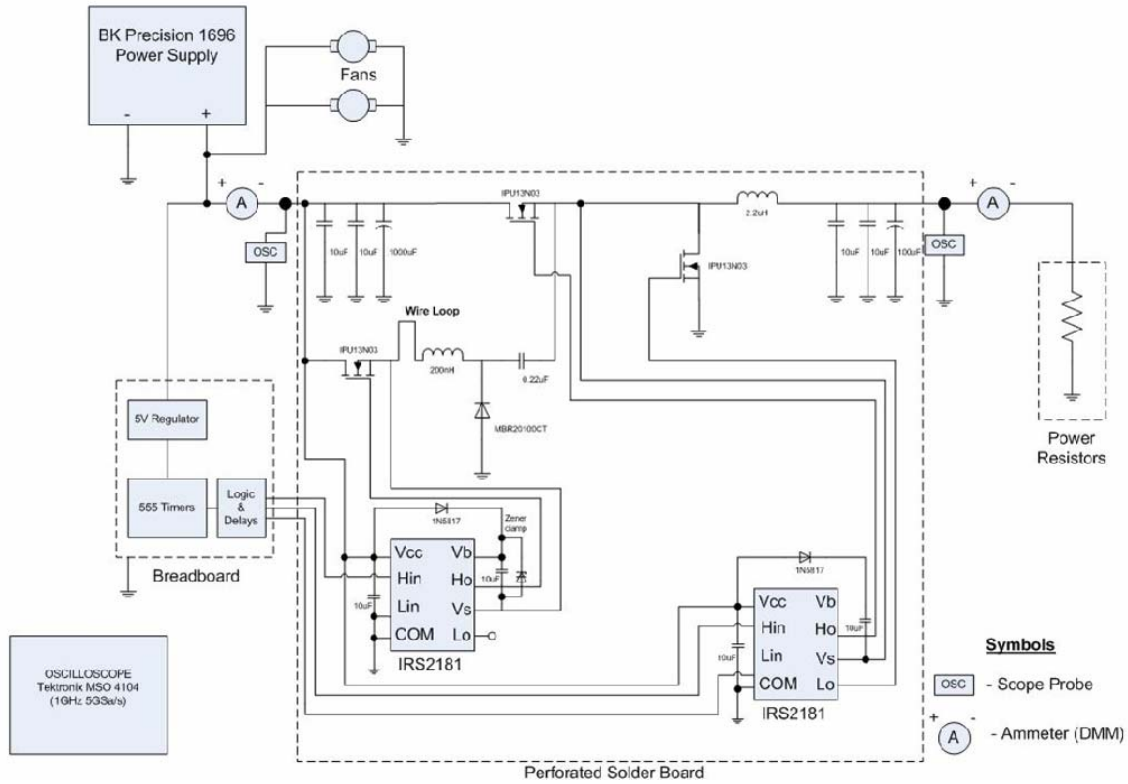


Figure 26: Synchronous ZVT Converter Test Setup

This setup differs somewhat from the others in that power resistors were used as the output load and a different oscilloscope was used in order to allow for current through the resonant inductor to be monitored (using the wire loop noted in the figure with a current probe). Below is a picture of the actual circuit that was built noting the input and output voltage test points.

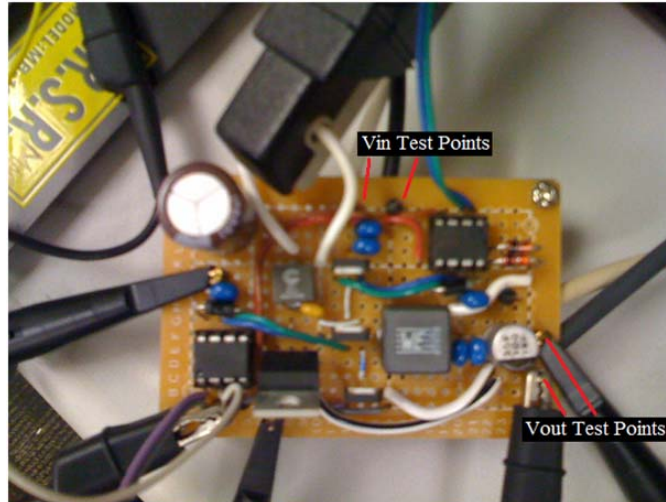


Figure 27: Synchronous ZVT Converter Board

The converters functionality was confirmed by monitoring the operational waveforms using the oscilloscope. Due to probe limitations all voltages shown are with respect to ground. The waveforms are labeled on the figure to the left.

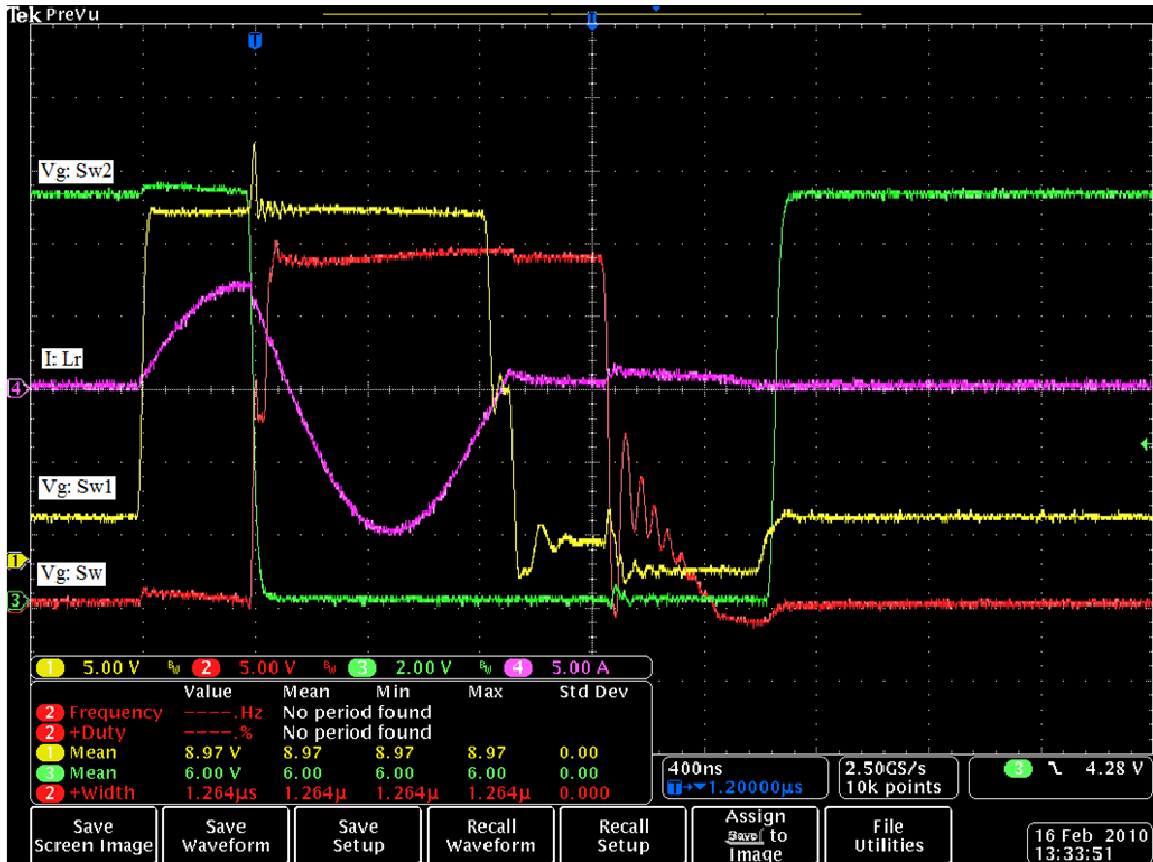
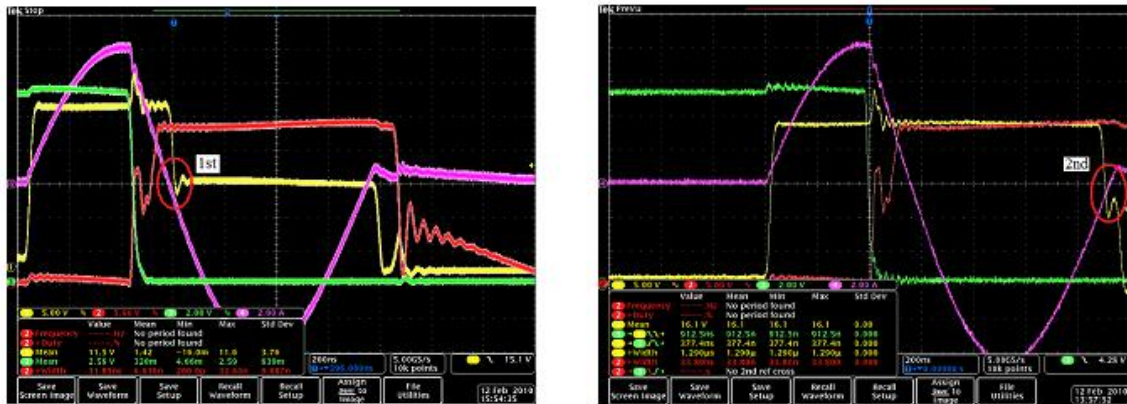


Figure 28: Synchronous ZVT Experimental Operational Waveforms

Given that this capture is taken for a 3A load current ZVS turn on of the main switch can be confirmed by the resonant inductor current level during switching since it is greater than the load current the body diode of the main switch must be conducting and thus achieving ZVS. ZCS turn on and off of the auxiliary switch is confirmed by the resonant inductor current waveform in comparison to the Vg Sw1 (aux switch), since switching occurs at zero current soft switching is confirmed for this switch as well. Another item of importance, the discharge of the resonance cap before the turn on of Sw2, can be seen using the Vg of the main switch. At the turn off of the main switch

there is a descending ramp in V_g voltage this ramp is an indicator of the resonance capacitors discharge to zero and the transfer of its stored energy to the output. These operational waveforms show consistency with the waveforms found in [1].

The difference in efficiency by delaying the turn off of the auxiliary switch until the second zero crossing was experimentally tested using the same output load (1A) in comparison to the first zero crossing. The waveforms of each instance are shown below.



First Zero Crossing

Second Zero Crossing

Figure 29: Auxiliary Switch ZCS Turn off Points

Table 1: $\Delta\eta$ Due to ZCS Turn off Point

Timing Comparison of Aux Switch ZCS							
Vin (OSC)	Iin (DMM)	Vout (OSC)	Iout (DMM)	Pin	Pout	Ploss	η
12.000 V	0.588 A	3.270 V	0.940 A	7.1 W	3.1 W	4.0 W	43.56%
12.000 V	0.634 A	3.270 V	0.940 A	7.6 W	3.1 W	4.5 W	40.40%

2nd pt
1st pt

Since the circuit is operating in DCM the efficiency above is very low, however the clear difference in power loss of 0.5 W can be seen confirming power loss savings made by switching on the second ZCS turn off point. This second ZCS switching point is used in all analysis to follow.

Experimental efficiency results were obtained and the synchronous ZVT efficiency was compared to the efficiency of the standard synchronous converter below.

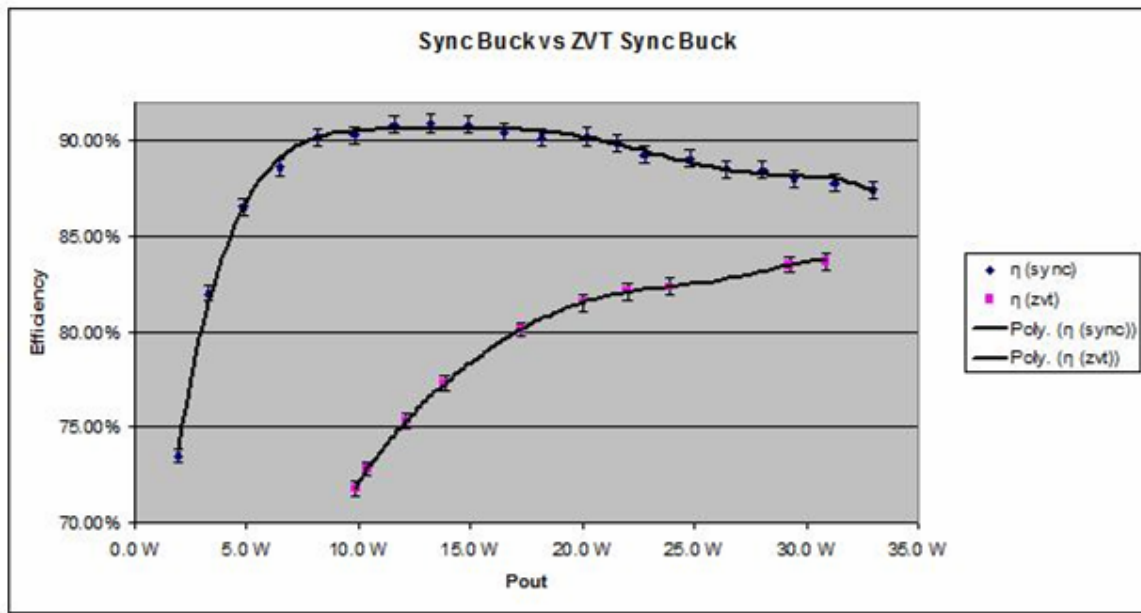


Figure 30: Synchronous ZVT vs. Synchronous buck Efficiency

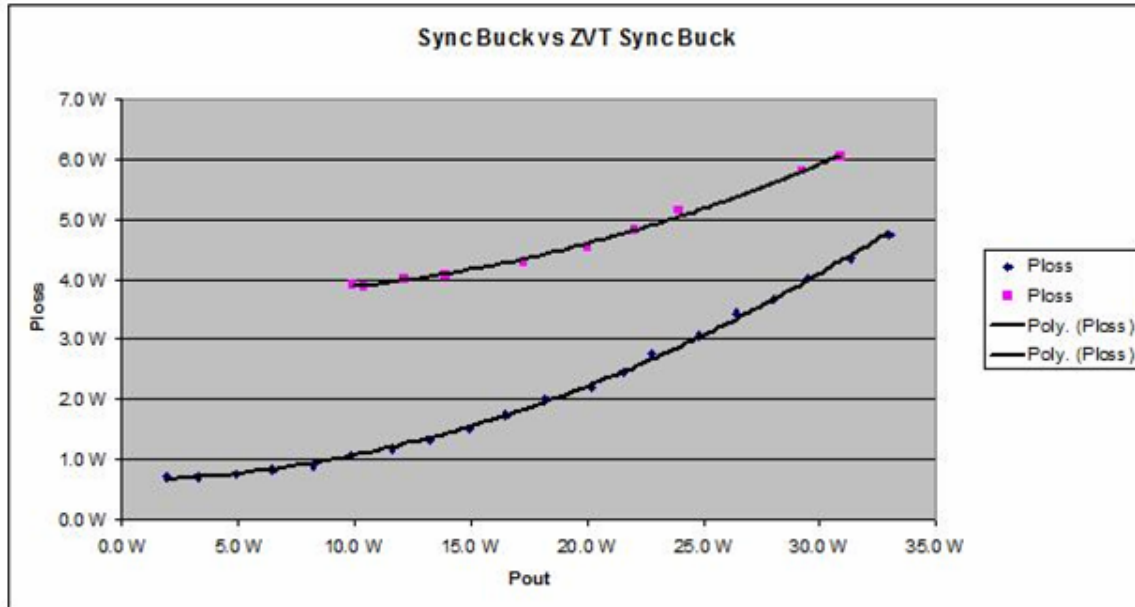


Figure 31: Synchronous ZVT vs. Synchronous buck Power Loss

The data above was taken for a switching frequency of 200 kHz for both converters. Obvious discrepancies are seen from what is expected in that the efficiency for the ZVT converter is lower than its hard switching counterpart. This could be due to several factors that will be discussed later. However, it appears as if there will be a crossover point at which the ZVT topology will become beneficial at higher output power level. The efficiency discrepancy was reduced somewhat by the improvement of the auxiliary components used. The first component change was the resonant capacitor. The capacitor used for the previous data was a class 2 type dielectric with a fair amount of ESR. This ESR can cause considerable loss given that the current ripple through this capacitor is quite large. So to reduce this loss a class 1 dielectric was used instead reducing the loss and improving the converters efficiency. The next component that was changed was the resonant inductor. Since the DC resistance of the inductor used was

already low an inductor with lower core losses was used to replace it. This also improved the converters efficiency. These auxiliary component improvements are reflected in the efficiency plots below.

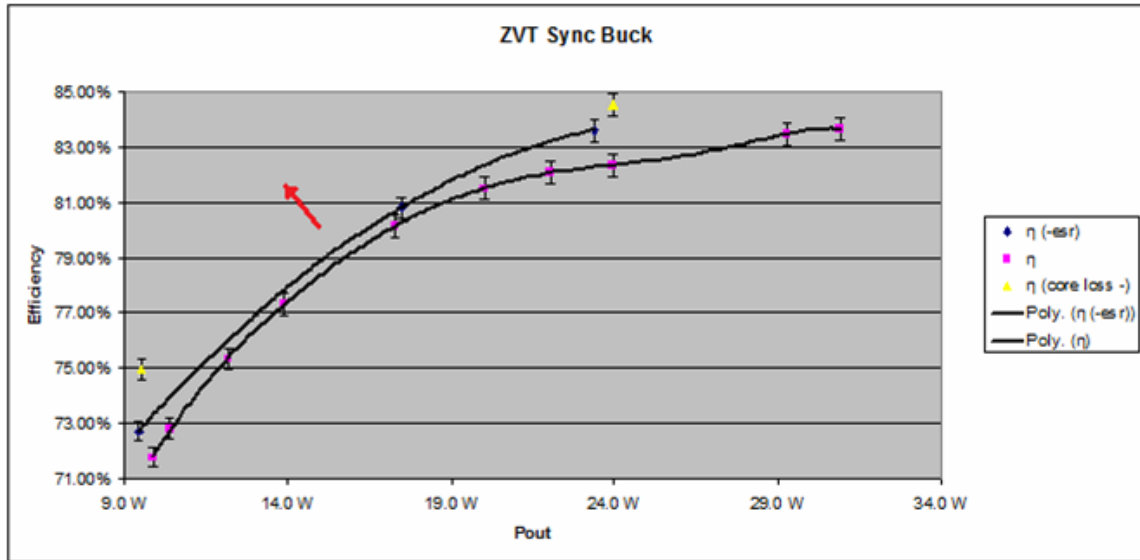


Figure 32: ZVT Efficiency with Auxiliary Component Improvement

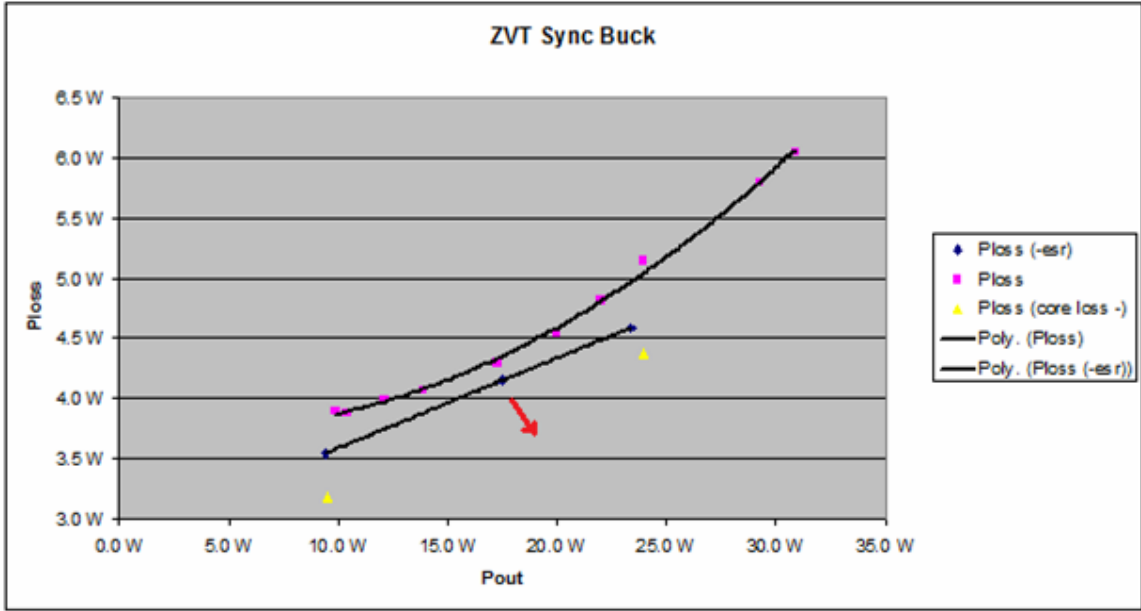


Figure 33: ZVT Power Loss with Auxiliary Component Improvement

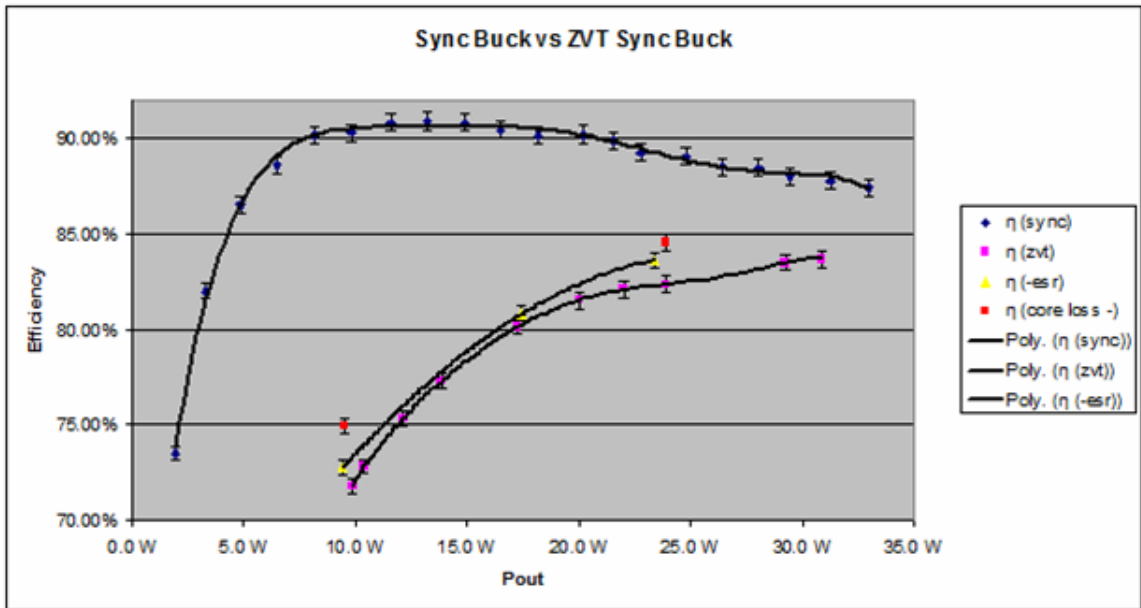


Figure 34: ZVT η Improvement in Reference to Synchronous Buck

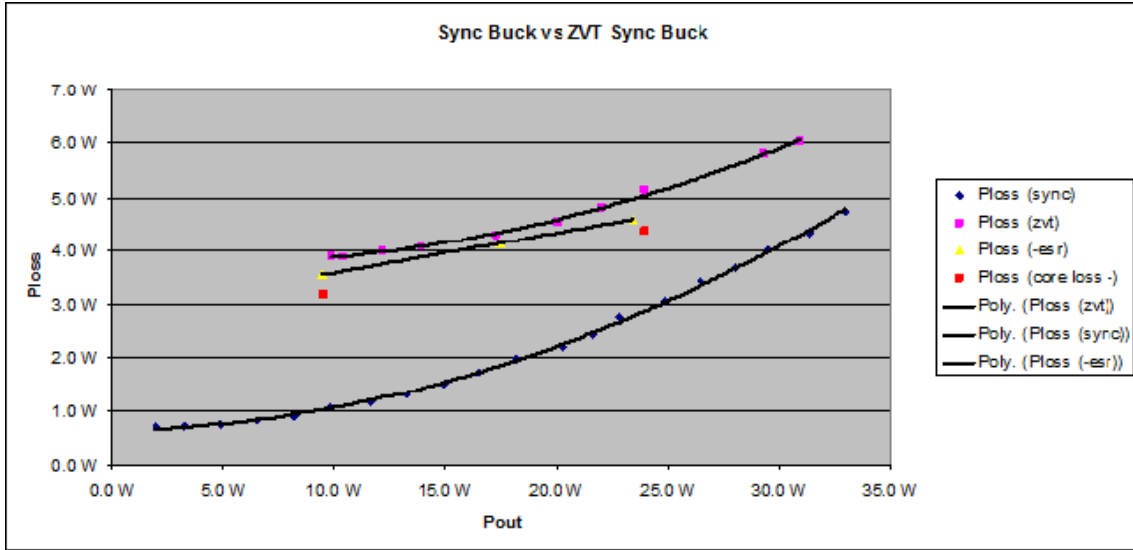


Figure 35: ZVT Ploss Improvement in Reference to Synchronous Buck

By improving the auxiliary components (i.e. reducing their losses) an overall power loss and efficiency improvement can be seen. It appears that the previously projected crossover point may happen earlier. In an attempt to analyze the location of the additional losses, power loss estimation by component can be done using the equations from chapter 2. The tables below are used to estimate some of the losses.

Table 2: Standard Synchronous Buck Converter Loss Estimation

<i>Sync Buck t_{dead}= 300ns</i>				
	High Side	Low Side	Lout	
	<i>IPU13N03</i>	<i>IPU13N03</i>	<i>732-2140</i>	total
Conduction Losses	0.032 W	0.082 W	0.027 W	0.141 W
Switching losses	0.095 W	0.350 W		0.445 W
				0.587 W
Other losses				0.513 W
total losses	0.127 W	0.432 W	0.027 W	1.1 W
			Pin	10.9 W
			Pout	9.8 W
			η	89.91%

Table 3: ZVT Synchronous Buck Converter Loss Estimation

<i>ZVT Sync Buck</i>							
	High Side	Low Side	Aux	Lr	Aux & Other	Lout	
	<i>IPU13N03</i>	<i>IPU13N03</i>				<i>732-2140</i>	
						total	
Conduction Losses	0.032 W	0.081 W	0.717 W	0.010 W		0.027 W	0.866 W
Switching losses							0.000 W
				0.130 W	2.904 W		0.996 W
Other losses							2.904 W
total losses	0.032 W	0.081 W	0.717 W	0.140 W		0.027 W	3.9 W
						Pin	13.8 W
						Pout	9.9 W
						η	71.74%

These tables are generated for a load of 3A. The ZVT loss estimations are for the unimproved converter. By estimating the losses in this fashion, it can be seen that in the ZVT converter there are a fair amount of losses that are not accounted for but can and most likely are attributed to additional auxiliary component loss.

3.5 Conclusions

Soft switching can be used to improve converter performance. However several factors come into play that can influence the benefits of soft switching. Examples of these factors are power semiconductor technology, switching frequency, and power range [30]. Based on the data obtained it seems that for the given components, switching frequency, load range, and other operating characteristics that the benefits of ZVT are outweighed by the additional losses induced. By operating at a fairly low switching frequency and using switching components that have inherently low switching losses, ZVT's benefits might be overshadowed at this load range. As stated previously, it appears that perhaps outside of this load range there may be benefits but due to measurement limitations a higher load range could not be tested. Another factor that could be contributing to the discrepancy in the efficiency data could be the length of the resonance period used in this design. The resonance period length could be reduced leading to smaller conduction losses and perhaps higher efficiencies. Although this converter does not prove beneficial over its standard hard switching counterpart this shows that several circuit factors, as stated in [30], can come into play when determining if ZVT will be of benefit for use.

Increasing the switching frequency should better show the benefits of this topology for a given set of components. In future testing, using components that allow for high frequency operation, much more aggressive switching frequencies can be tested and the results at these higher frequencies can be compared to give indication of this topologies potential usefulness in applications such as integration. In the next section there is some discussion about integrated converter applications and this topologies potential in such applications.

3.6 Integrated Converter Discussion

The demand for converters to shrink further and further in size has brought on several new converter designs that are completely on chip [14] [24-26] or vary near to totally on chip [27]. These converters operate at extremely high frequencies when compared to their discrete component counterparts. This high frequency is sure to cause some fairly significant switching loss. Since frequencies are sometimes very high ZVS transitions can sometimes come for free, so to speak, since the intrinsic parallel capacitance of the devices can cause ZVS turn off conditions. This depends greatly on the individual case. Turn on, on the other hand is still typically hard switching so this leaves room for improvement. Although this room for improvement can be filled by topologies such as the ZVT topology mentioned in [1], there are other complications that may offset any benefits of using a topology such as this in integrated applications, namely front end device losses [25]. Front end device loss has only been mentioned in passing up to this point because at lower frequencies this loss is rather insignificant. Front end loss refers to the losses incurred by driving the device gate. These losses occur in the gate driver as well as in the MOSFET gate itself. In order to drive the gate both high and low the gate capacitance is charged and discharged through finite resistance values. The rapid charge and discharge of gate capacitances can cause significant energy loss even for fairly small gate capacitances. Since the topology presented in [1] has more active devices that must tolerate power stage level stresses, losses such as these may prove problematic depending on how high the switching frequency is for the converter. Depending on the frequency

and components, operating at the typical light loads associated with integrated converters may also prove problematic for maximizing ZVT's benefits. The light loads due to limitations of current are typically set by current density limitations due to conductor thickness in integrated inductors. As such the more pressing issues for fully integrated converters may be found in the output inductor. Topologies that use interleaving of inductors can partially aid in this dilemma [24] [29].

The issues in the full integration of buck converters are numerous and several solutions are being offered by newer topologies. However it seems that integrated converters will always be fundamentally limited in their ability to deliver large amounts of power but it is not to be said that there is no room for improvement. Topologies using ZVT methods should not be counted out for potential use in the improvement of such converters.

CHAPTER 4: NON-ISOLATED SYNCHRONOUS BUCK CONVERTER STRESS EFFECTS

4.1 Introduction

In this chapter the focus is shifted to a much different issue than the previous chapter. The issue of device ageing effects on standard non-isolated synchronous buck converters will be explored in detail. Device ageing and device stress are directly related. By controlling the stress applied on a device one can control the rate at which a device degrades. Increasing the stress in the appropriate manner can be used as a tool to theoretically project normal degradation over long periods of time (ageing effects). The main goal in this chapter is to illustrate how a method of this type may be used for showing the effects that MOSFET ageing can have on power electronic circuits, specifically synchronous buck converters.

In order to effectively accomplish this goal, first some background information about hot carrier effects will be mentioned. Then the converters operational characteristics effect on the converters susceptibility to ageing effects will be mentioned as well. The methods used in an attempt to experimentally confirm the theory in this chapter will be described in detail. Finally the results for both experimentation as well as simulation will be shown and conclusions about this data will be made.

4.2 Hot Electron Device Degradation

4.2.1 Description

Hot carrier degradation at the device level has been fairly well documented and experimental validation of this theory has been performed [5] [7-10]. The magnitude and impacts of this degradation on circuit level applications have been studied for digital circuits and some analog applications such as RF circuitry in the past [6]. Only recently has consideration been turned to possible effects on power electronics applications such as switching mode power supplies like buck converters [4]. Before moving to the higher level effects and experimental results, some description of the theory is in order.

The following description applies to the traditional lateral MOSFET structure. The mechanisms that cause device degradation for the traditional MOSFET structure are fairly simple to explain and understand given a basic knowledge of semiconductor devices. To explain these mechanisms the figure below will be used for reference. Hot carriers actually degrade MOSFETs with the combined effects of two mechanisms, damage to the oxide-substrate interface causing lower mobility at the surface region and creation of trapped charge. Given the following conditions for an nmos, $V_{gs} > V_{th}$ so that a channel is formed beneath the oxide and $V_{ds} > 0V$ so that current will flow from drain to source ($I_d > 0A$), it is possible for hot electron degradation to occur on some level. However, effects are greatly dependent on the magnitude and direction of the electric field in the device. The effects are greatest when V_{gs} is large relative to V_{th} and

close to the value of V_{ds} so the electric field looks somewhat like in the figure below. The horizontal component of the electric field is the desired component, in that it causes carriers (electrons) to flow from source to drain. The vertical component is necessary to create the channel in the first place but has a secondary undesired effect. The vertical component of the electric field tends to cause the carriers, electrons in this case, to stay near the surface at the oxide interface increasing the chance of interfacial lattice damage as well as the chances that an electron will have enough energy to exceed the energy barrier necessary to enter the oxide [7]. When an electron enters the oxide it will either be swept to the gate by the electric field causing gate current or become trapped at neutral centers in the oxide causing oxide charging [6] [7]. Both interface damage and trapped charge create changes in devices characteristics that are described in the next section.

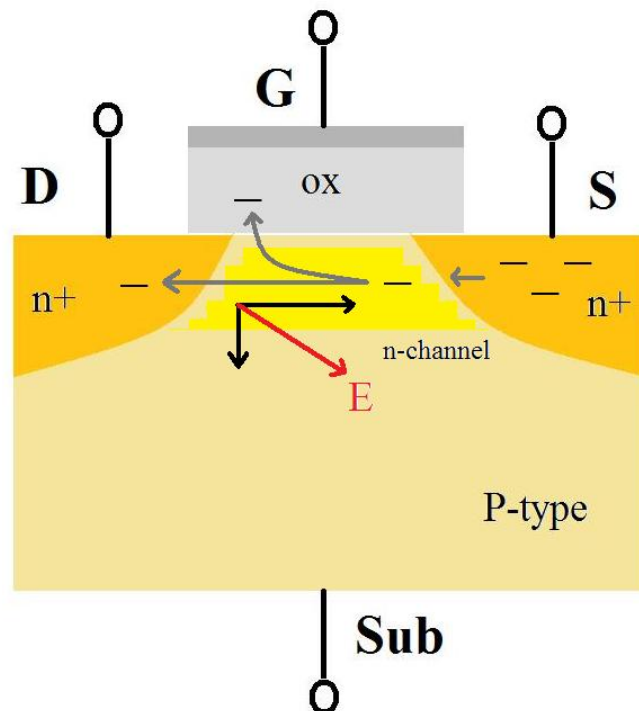


Figure 36: Oxide Electron Trapping for Traditional MOSFET Structure

4.2.2 Effects on Device Characteristics

Interface damage and trapped charge create changes in device characteristics that can be undesirable for circuit operation. As mentioned previously interface damage lowers the carrier mobility at the surface near the interface. The surface damage tends to increase the channels effective resistance by partially impeding the carrier's path through the channel along the interface. Trapped charge in the oxide will cause changes in V_{th} , the direction of the change depends on the type of carriers that are injected into the oxide, hot electrons or hot holes. In the case of nmos shown in the figure above hot electrons are injected in the oxide, this injection effect is also referred to as oxide charging. Oxide charging in the case of hot electron injection will cause V_{th} to increase. This trapped negative charge tends increase the gate charge for a given bias condition increasing the gate capacitance values, such as the gate to source capacitance. The figure below illustrates the effects mentioned on a standard MOSFET cross section by showing the device at a given biasing condition before (left) and after (right) hot carrier ageing.

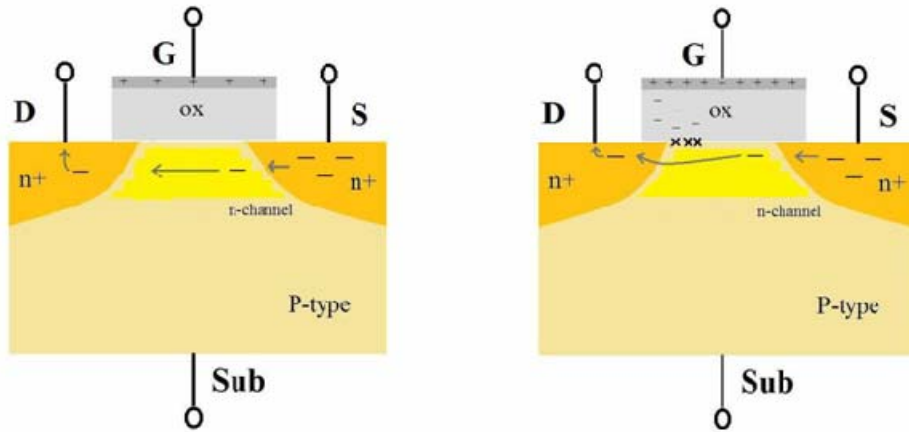


Figure 37: MOSFET Before and After Hot Carrier Ageing

Although the effects may vary and be slightly more complex the same overall concepts still apply to more recently used device architectures such as LDMOS. An example of a general LDMOS structure before and after ageing is shown below.

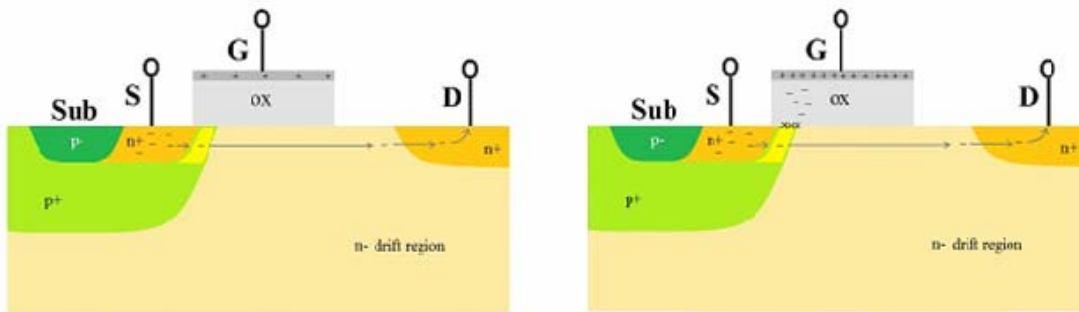


Figure 38: LDMOS Before and After Hot Carrier Ageing

4.2.3 Effects Pertaining to Power Electronic Circuits

With switching mode power supplies aside from reliability and proper regulation often high efficiency is paramount. Since power efficiency is generally important it is desirable to keep component losses to a minimum. Keeping this in mind, much of the time a large portion of the total losses of a converter can be found in the switching devices such as MOSFETs. This makes the switching device of key importance to converter design. So, it logically follows that degradation in device characteristics that cause additional losses should result in circuit efficiency degradation. If the effects are confirmed, it then becomes a question of how much degradation occurs.

Focusing in on power losses due to MOSFET devices in power converter applications, as stated previously one can find two main categories of losses, conduction losses and switching losses. Since for switching converters the MOSFET is typically trying to fill the role of an ideal switch there are two modes generally, on and off. For MOSFETs, conduction losses occur when the switch is turned on. Conduction losses for MOSFET devices is mainly caused by $R_{ds(on)}$ or effective resistance of the device during conduction (equations 6 & 7). Switching losses are losses that occur during the switches transition from off to on and vice versa. Switching losses can be comprised of a combination of different effects caused by the MOSFETs characteristics and circuit conditions but in general switching losses are highly influenced by the devices gate charge (as in equations 8 & 11). Since hot carrier ageing can affect both $R_{ds(on)}$ and Q_g it is worth investigating device ageing effects for switching power supplies.

4.2.4 Power Device Structures

It should be mentioned that MOSFET structures vary widely and structures used can be highly application dependent. Device structure is very important when talking about hot carrier effects. The actual MOSFET structures of the devices typically used in power converter applications differ from the traditional structure talked about above. For several reasons vertical devices such as VDMOS are used for converter applications [11] [12]. These types of structures have the benefits that traditional MOSFETs have to offer with additional benefits such as high current capability and fairly high blocking voltage. Below is a basic example of a vertical structure like the one found in [10].

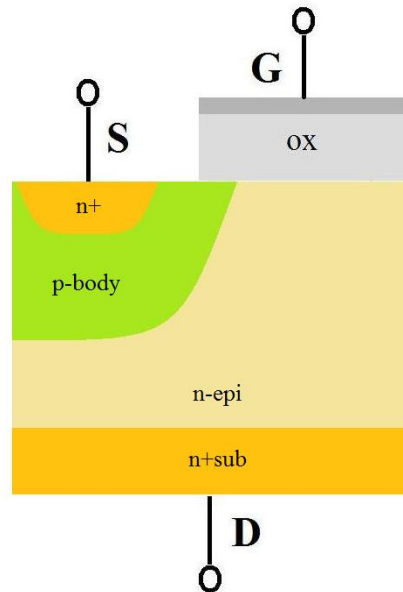


Figure 39: Example VDMOS Structure

Vertical device structures are typically considered to be fairly immune to hot electron ageing since the flow of carriers is in the vertical direction and mostly avoids the oxide silicon interface. However there have been studies showing that at least some of these structures can show degradation due to the hot electron effect [10]. This is an important thing to consider since vertical silicon devices are prominent in applications such as the synchronous buck converter. They are used not only for the benefits offered but also since they are mature technology. Other newer technologies are being developed such as GaN HEMTs [13]. These and other non-silicon technologies may see more widespread use in the future but for now, especially for integrated applications, silicon based technology is dominate.

4.2.5 Modeling/ Simulating Effects

Although the impact of ageing may vary with device structure, modeling can be done similarly for all structures since it is the overall device characteristic changes that are of concern. The non-isolated synchronous buck converter is a good topology to look at for this investigation since it is such a widely used and easy to implement topology. The following sections will be specifically focusing on the synchronous buck converter. As was mentioned before, this is a well known and widely used topology, which makes it a good choice for use in this study. Nmos devices are typically the switching element of choice for this converter topology. As went over in chapter 2, power losses can be estimated using some key parameters from the MOSFET [2].

Modeling the effects of hot electron ageing can be done both at the device and circuit level fairly easily. At the device level, the parameters that are affected can be modified in the model. The two parameters to adjust are V_t (threshold voltage) and μ (carrier mobility). By changing these parameters appropriately, device ageing can be modeled. This device model can then be used in circuit to compare the losses before and after device ageing. If access to these parameters is unavailable it is possible to at least partially model simulate these changes using circuit conditions alone. Simulation such as the latter will be used for obtaining results in the sections to follow.

4.3 Susceptibility of Converters

In order to determine if a converter's efficiency is susceptible to ageing effects, the switching device used must show hot electron ageing susceptibility and the converter itself must operate such that the level of degradation developed in the device has a significant effect on the level of power loss in the converter. In short both device and circuit must be susceptible to degradation. To clarify what is meant by this some more explanation is needed.

Device susceptibility, as mentioned previously, is structure dependent as well as biasing dependent. Some structures are highly resistant to ageing effects while others tend to degrade more easily. Lateral devices with the oxide silicon interface parallel to carrier flow are typically more susceptible to degradation. Lateral structures such as these are not typically used for converters except for some novel cases with integration in mind [14]. Vertical structures typically used tend to be less susceptible but can degrade

similarly [10]. If devices are robust to ageing then it is less likely that significant changes in efficiency will occur for a given converter. On the other hand, if the devices do show degradation efficiency change becomes more circuit level dependent.

Circuit level converter characteristics can play a key role in a converter's overall susceptibility to ageing. Switching frequency, load current, voltage step, and output power are converter characteristics that can affect the susceptibility of a converter to device degradation. A gate charge increase for example has greater effects at higher switching frequencies. $R_{ds(on)}$ changes will have greater effects if load current is high. Other factors play a role in how much efficiency may or may not be changed. An example using simulation shows how some of these factors can increase or decrease the impact of $R_{ds(on)}$ change.

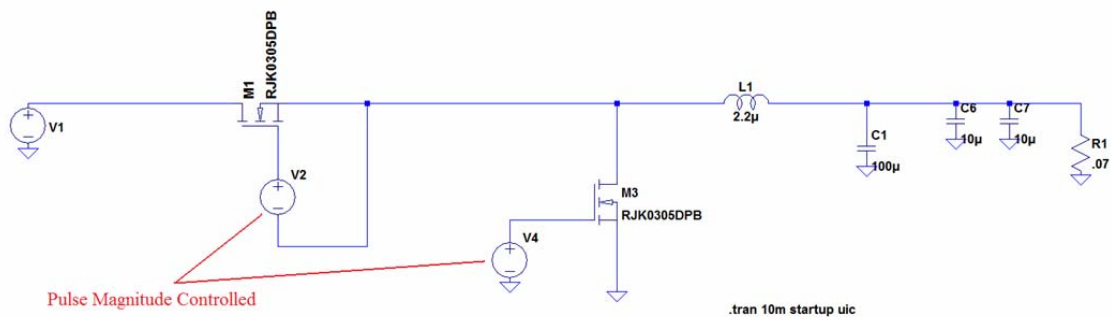


Figure 40: Synchronous Buck Circuit for $\Delta R_{ds(on)}$ Simulation

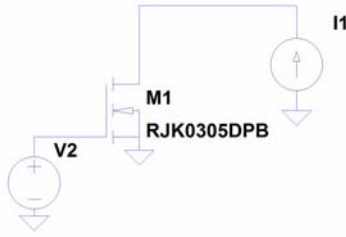


Figure 41: Rds(on) Measurement Simulation Circuit

Simulation was done using LTSpice in order to show how converter characteristics can effect a given change in Rds(on) effect on efficiency. Different pulse magnitudes were used as Vgs gate drives in order to achieve different Rds(on) values. The Rds(on) was changed by 20% for each simulation shown in the table below. Rds(on) was measured using a sub circuit simulation. As shown in the table converters with high current relative to Vout and larger impacts of conduction loss will have greater efficiency changes for a given Rds(on) change.

Table 4: Simulated $\Delta R_{ds(on)}$ Impact on Efficiencies

Converter	Rds(on) (mΩ)	Vgs	Pout	Ploss (total)	η	ΔP_{loss} (mW)	$\Delta \eta$	
5V to 0.7V	5.84	12.0 V	7.060 W	1.534 W	82.15%	131	-1.17%	10A Load
	7.04	8.7 V	7.089 W	1.665 W	80.98%			
12V to 3.3V	5.84	12.0 V	33.186 W	1.659 W	95.24%	174	-0.48%	
	7.04	8.7 V	33.174 W	1.833 W	94.76%			
	5.84	12.0 V	10.244 W	0.306 W	97.10%	30	-0.27%	3A Load
	7.04	8.7 V	10.246 W	0.336 W	96.82%			

This example illustrates that although a device's $R_{ds(on)}$ might degrade greatly a measurable change in efficiency may or may not manifest itself depending on the converters sensitivity to this change.

4.4 Experimental Simulation of Device Ageing

4.4.1 Methods of Stressing

In order to attempt to experimentally induce accelerated ageing voltage stresses that are much higher than the typical must be applied to the MOSFET devices in an attempt to create a high internal electric field. Methods of stressing and there actual effects on the device become somewhat difficult to identify when using off the shelf discrete MOSFET parts as was done to follow but with the simple goal of inducing some measurable device $R_{ds(on)}$ degradation in mind stressing experimentation was carried out. However it was unknown whether any results showing degradation would occur and not knowing device cross sections proves problematic to this goal.

4.4.2 Out of Circuit Stressing

The most controlled method of stressing was out of circuit testing in which the device was stressed separately from the synchronous buck converter in order to achieve a measurable $R_{ds(on)}$ change and then replaced in circuit to show its effects on efficiency (similar to stressing performed in [10]). Two devices have been stressed using this

method IRLB8748 and STP22NF03L. The individual MOSFETs were connected as below.

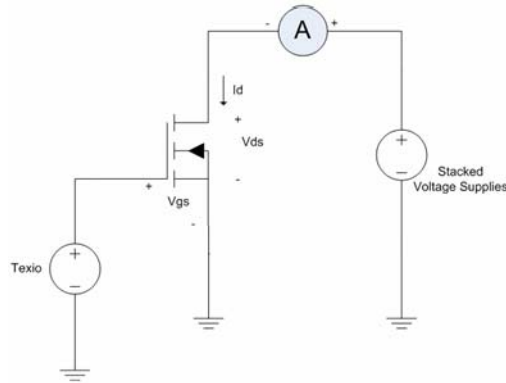


Figure 42: MOSFET Out of Circuit Stressing

By applying a V_{ds} voltage that is large (larger than rated V_{dss}) the hope was to induce hot carrier effects and cause device degradation. To try to induce these effects both V_{ds} and V_{gs} were adjusted to higher and higher values while remaining at power dissipation levels tolerable by the device. A V_{ds} at which avalanche current was induced was used as a benchmark for high V_{ds} . Several stressing intervals were used, both before and after each interval the devices $R_{ds(on)}$ was monitored for various drain current and gate voltages. The measurement of $R_{ds(on)}$ was taken using the circuit below.

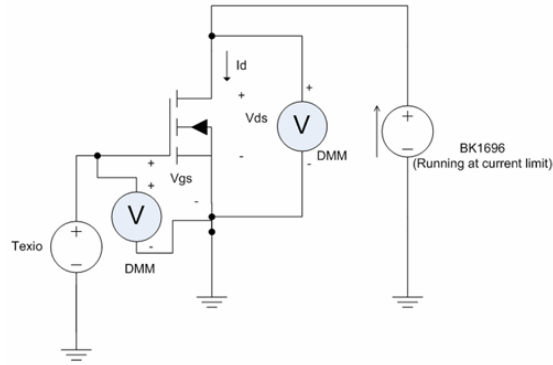


Figure 43: Device $R_{ds(on)}$ Measurement Circuit

4.4.3 *In Circuit Stressing*

In circuit stress testing was also used to try to induce device degradation and in turn circuit efficiency degradation. This method, albeit less controlled, was intended to stress the device with the transient effects that are seen in converter operation. This method separated circuit operation into to modes of operation normal and stress operation. Normal operation was used as an example of a typical converter operation. Stress operation used a very high input voltage near the V_{ds} breakdown voltage for the high side device. In this case it was the circuit's efficiency that was monitored between stressing intervals. The figure below shows the converter as it was connected for stressing operation.

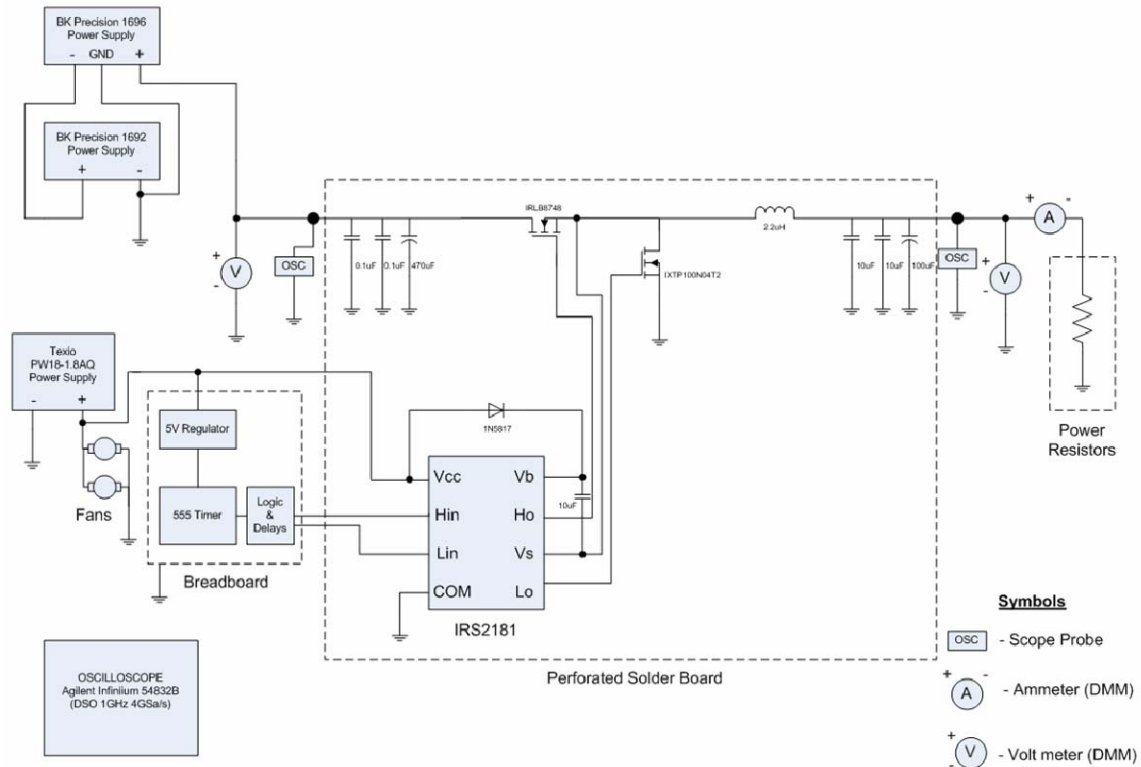


Figure 44: In Circuit Stressing Setup

4.5 Results/ Conclusions

The first method of stressing that was tested was in circuit testing. For this testing the converter was operating at a switching frequency of 200 kHz and tdeadtime was 100 ns. Initial η vs Pout set of data was taken for various output power levels. Two converter voltage steps were monitored 12V to 3.3V and 5V to 3.3V for their efficiencies at a load of 3.8A. These efficiency points were monitored between stressing intervals to look for any changes due to stressing effects. Only the high side device was stressed (IRLB8748) in this scenario since a more robust device (higher Vdss) was used for the low side device

(IXTP100N04T2). The high side device's breakdown voltage was measured prior to stressing and was found to be approximately 31.2V. Many stressing intervals were used incrementing the input voltage each time. The maximum level of stress applied was 32.5V for a time period of 60 minutes using a stressing operation duty cycle of 10% with a load current of 0.33A. Stressing using this method was found to be ineffective, at least for the scenarios that were tested. The efficiency of the converter never changed out of the experimental error. This method, although trying to mimic the actual circuit operation of the converter, is not particularly accurate to the types of stressing that may actually occur in the devices over time. For this reason continued stress testing was done out of circuit. For this testing there are also issues with the converters level of sensitivity to changes in Rds(on) as shown in the table below.

Table 5: Theoretical $\Delta\eta$ due to $\Delta R_{ds(on)}$

<i>High Side switch change only</i>								
Converter	Rds(on) (mΩ)	Vgs	Pout	Ploss (Rds(on))	Ploss (total)	η	ΔP_{loss} (mW)	$\Delta\eta$
5V to 3.3V	4.80	11.0 V	12.470 W	0.045 W	0.983 W	92.69%	9	-0.06%
	5.76	11.0 V	12.470 W	0.054 W	0.992 W	92.63%		
12V to 3.3V	4.80	11.0 V	12.380 W	0.019 W	1.567 W	88.76%	4	-0.02%
	5.76	11.0 V	12.380 W	0.023 W	1.571 W	88.74%		
<i>*yellow highlights experimental data</i>								

3.8A Load

This table uses the actual experimentally measured efficiency and power loss data and the estimated loss due to Rds(on) and projects the effects of an increase of 20% in Rds(on). As can be seen in the table the change in efficiency would be minimal. This result is insensitive to $\Delta R_{ds(on)}$ showing insignificant efficiency changes due to Rds(on).

However, in a more positive light this result shows that a converter of this type would be very robust to any changes in $R_{ds(on)}$ if they did occur.

With circuit susceptibility being a factor the converter characteristics were changed to a 5V to 0.7V with a load of 10A. This converter showed susceptibility to $R_{ds(on)}$ changes in simulation and could prove useful in showing efficiency changes better. In order to assure that $R_{ds(on)}$ was indeed changing a more direct out of circuit approach is needed.

After in circuit stress testing proved ineffective in inducing degradation the approach of out of circuit testing was taken. The previous device used in circuit (IRLB8748) was stressed out of circuit as well using the method stated in the above section. Its $R_{ds(on)}$ was measured for several different gate voltages and drain currents prior to and after stressing intervals. Several stress intervals were applied to this device. For this device and method no significant degradation was seen outside of experimental measurement error. A second device (STP22NF03L) was also stressed similarly. This device's breakdown voltage was found experimentally to be approximately 35.4V. Again several stress intervals were impressed upon this device. The maximum stress interval applied to this device was a V_{ds} of 36V at a V_{gs} of 2V with $I_d = 30$ mA for a time interval of 12 hrs. As can be seen in the table below no significant changes occurred in the $R_{ds(on)}$ of this device either, as all changes are inside experimental error.

Table 6: Rds(on) Before and After Stress (STP22NF03L)

<i>Low Side switch</i>		
<i>Before</i>	<i>After</i>	
Rds(on) (mΩ)	Rds(on) (mΩ)	Vgs
2248.00	2224.00	2.8 V
392.00	390.25	3.0 V
66.45	66.33	3.5 V
45.83	45.90	4.0 V
38.23	38.20	5.0 V
33.13	32.96	10.0 V

As stated previously the effectiveness of stressing methods is difficult to analyze correctly without knowing the specific device architecture. With the given, off the self devices, and the methods used no degradation was able to be produced. This indicates that either the devices are robust to hot electron effects or the methods of stressing were ineffective. For vertical devices it is typically accepted that there is immunity or at least a very high level of resistance to hot electron effects. Vertical symmetrical structures such as the ones found in [11] can be particularly resistant to hot electron effects due to the reduction of localized high electric field. At least some vertical devices have displayed some susceptibility to hot electron effects [10] and with this in mind further investigation may prove useful. Using different devices and perhaps adjusted methodology, the hot electron effect may still have effects on some converters.

CHAPTER 5: CONCLUSIONS AND FUTURE WORK

5.1 Conclusions

In this thesis current topics relevant to buck converters have been brought up and addressed through theory, simulation, and experimentation. Two specific topics were focused on, ZVT topology analysis and possible future uses such as integration and the possible effects due to long term converter stressing. Thus far framework for continued study of ZVT's potential for integration has been laid down. Experimental testing using a discrete approach was done for this topology leaving further study of more aggressive switching frequencies typical for integration open to continue. Converter stress effects have been gone over and discussed thoroughly. Although theory may suggest a window of possibility for these effects to occur, experimentation has yet to reveal any possible threats to converter performance. The potential for these effects has yet to be proven. Future work in both topics is of interest.

5.2 Future Work

Future work may include continued study and testing of ZVT topologies specific to integration (i.e. very high frequency and components smaller in size). Also, continued study of converter stressing to either confirm or deny the presence of significant ageing effects in buck converters.

REFERENCES

- [1] S. Pattnaik, A. K. Panda, Aroul K., K. K. Mahaptara, "Experimental Validation of A Novel Zero Voltage Transition Synchronous Buck Converter," in Proc. TENCON 2008 IEEE Region 10 Conf. 2008, pp. 1-6.
- [2] Jon Klein, "Synchronous buck MOSFET loss calculations with Excel model," Product and Technical Information/ Design Resources www.fairchildsemi.com , January 4, 2006
- [3] I. Batarseh: *Power Electronic Circuits*, John Wiley & Sons, New York, 2004.
- [4] J. S. Yuan, "Evaluation of Hot-Electron Effect on LDMOS Device and Circuit Performances," IEEE Transactions on Electron Devices, Vol. 55, No. 6, June 2008
- [5] H. Wang, M. Davis, H. De, S. Bibyk, Y. Nissan-Cohen, "Transient Hot-Electron Effect on N-Channel Device Degradation," IEEE Conf. 1989, pp. 79-82.
- [6] R. J. Baker: *CMOS Circuit Design, Layout, and Simulation*, Revised Second Edition, John Wiley & Sons, Hoboken, New Jersey, 2008.
- [7] R. F. Pierret: *Semiconductor Device Fundamentals*, Addison-Wesley, 1996.
- [8] S. L. Von Bruns, R. L. Anderson, "Hot Electron-Induced Interface State Generation in n-Channel MOSFET's at 77K," IEEE Transactions on Electron Devices, Vol. ED-34, NO. 1, January 1987.
- [9] R. Versari, A. Pieracci, "Experimental Study of Hot-Carrier Effects in LDMOS Transistors," IEEE Transactions on Electron Devices, Vol. 46, NO. 6, June 1999.
- [10] P. Moens, G. Van den bosch, G. Groeseneken, D. Bolognesi, "A Unified Hot Carrier Degradation Model for Integrated Lateral and Vertical nDMOS Transistors," in Proc. ISPSD '03. 2003 IEEE 15th International Symposium on, Power Semiconductor Devices and IC's. 2003, pp. 88-91.
- [11] H. P. E. Xu, O. P. Trescases, I. -S. M. Sun, D. Lee, W. T. Ng, K. Fukumoto, A. Ishikawa, Y. Furukawa, H. Imai, T. Naito, N. Sato, S. Tamura, K. Takasuka, T. Kohno, "Design of a rugged 60 V VDMOS transistor," IET Circuits Devices Syst., 2007, 1, (5), pp. 327-331.
- [12] B. Jayant Baliga, "Trends in Power Semiconductor Devices," IEEE Transactions on Electron Devices, Vol. 43, NO. 10, October 1996.

- [13] W. Saito, T. Nitta, Y. Kakiuchi, Y. Saito, K. Tsuda, I. Omura, M. Yamaguchi, "A 120-W Boost Converter Operation Using a High-Voltage GaN-HEMT," *IEEE Electron Device Letters*, Vol. 29, NO. 1, January 2008.
- [14] A. Emira, F. Carr, H. Elwan, R. H. Mekky, "High Voltage Tolerant Integrated Buck Converter in 65nm 2.5V CMOS," *ISCAS 2009, IEEE International Symposium on, Circuits and Systems*, 2009, pp. 2405 – 2408.
- [15] G. Hua, C.-S. Leu, Y. Jiang, F. C. T. Lee, "Novel Zero-Voltage-Transition PWM Converters," *IEEE Transactions on Power Electronics*, Vol. 9, NO. 2, March 1994.
- [16] K.-H. Liu, F. C. Y. Lee, "Zero-Voltage Switching Technique in DC/DC Converters," *IEEE Transactions on Power Electronics*, Vol. 5, NO. 3, July 1990.
- [17] W. Huang, X. Gao, S. Bassan, G. Moschopoulos, "Novel dual auxiliary circuits for ZVT-PWM converters," *Can. J. Elect. Comput. Eng.*, Vol. 33, NO. 3/4, Summer/Fall 2008.
- [18] E. Adib, H. Farzanehfard, "Family of isolated zero-voltage transition PWM converters," *IET Power Electron.*, 2008, Vol. 1, NO. 1, pp. 144-153.
- [19] E. Adib, H. Farzanehfard, "Zero-Voltage-Transition PWM Converters With Synchronous Rectifier," *IEEE Transactions on Power Electronics*, Vol. 25, NO. 1, January 2010.
- [20] E. Adib, H. Farzanehfard, "New Zero Voltage Transition PWM Converters," *ICIT2006, IEEE International Conference on, Industrial Technology*, 2006, pp. 801-806.
- [21] S. Pattnaik, A. K. Panda, K. K. Mahapatra, "Efficiency Improvement of Synchronous Buck Converter by New Passive Auxiliary Circuit," *TENCON 2008, IEEE Region 10 Conference*, 2008, pp. 1-6.
- [22] L. Shi, L. Chen, C. Yin, "A Novel PWM Soft Switching DC-DC Converter," *INTELEC '06, 28th Annual International, Telecommunications Energy Conf.*, 2006, pp. 1-6.
- [23] M. L. Martins, H. Pinheiro, J. R. Pinheiro, H.A. Gründling, H.L. Hey, "Family of improved ZVT PWM converters using a self-commutated auxiliary network," *IEE Proc.-Electr. Power Appl.*, Vol. 150, NO. 6, November 2003.
- [24] J. Wibben, R. Harjani, "A High-Efficiency DC-DC Converter Using 2 nH Integrated Inductors," *IEEE Journal of Solid-State Circuits*, Vol. 43, NO. 4, April 2008.

- [25] M. Alimadadi, S. Sheikhaei, G. Lemieux, S. Mirabbasi, W. G. Dunford, P. R. Palmer, "A Fully Integrated 660 MHz Low-Swing Energy-Recycling DC-DC Converter," IEEE Transactions on Power Electronics, Vol. 24, NO. 6, June 2009.
- [26] W.-R. Liou, M.-L. Yeh, Y. L. Kuo, "A High Efficiency Dual-Mode Buck Converter IC For Portable Applications," IEEE Transactions on Power Electronics, Vol. 23, NO. 2, March 2008.
- [27] N. Wang, T. O'Donnell, R. Meere, F. M. F. Rhen, S. Roy, S. C. O'Mathuna, "Thin-Film-Integrated Power Inductor on Si and Its Performance in a 8-Mhz Buck Converter," IEEE Transactions on Magnetics, Vol. 44, NO. 11, November 2008.
- [28] Y.-C. Chuang, Y.-L. Ke, "High-Efficiency and Low-Stress ZVT-PWM DC-to-DC Converter for Battery Charger," IEEE Transactions on Industrial Electronics, Vol. 55, NO. 8, August 2008.
- [29] W. Li, X. He, "A Family of Isolated Interleaved Boost and Buck Converters With Winding-Cross-Coupled Inductors," IEEE Transactions on Power Electronics, Vol. 23, NO. 6, November 2008.
- [30] M. L. Martins, J. L. Russi, H. L. Hey, "Zero-voltage transition PWM converters: a classification methodology," IEE Proc.-Electr. Power Appl. Vol. 152, NO. 2, March 2005.
- [31] T. Dyer, J. McGinty, A. Strachan, C. Bulucea, "Monolithic Integration of Trench Vertical DMOS (VDMOS) Power Transistors into a BCD Process," Proc. ISPSD '05, The 17th International Symposium on, Power Semiconductor Devices and IC's, 2005, pp. 47-50.
- [32] P. T. Krein: *Elements of Power Electronics*, Oxford University Press, New York, NY, 1998.